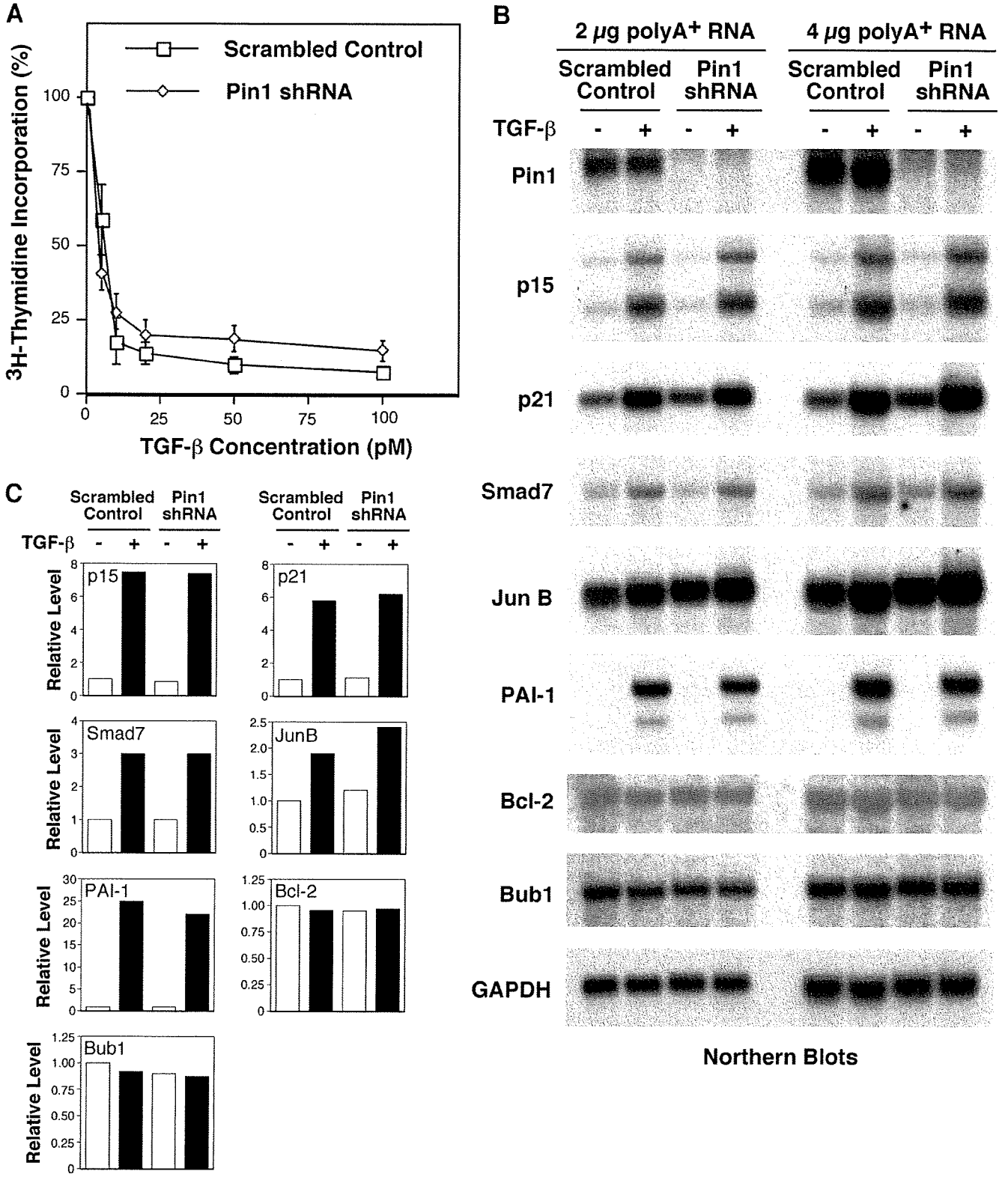

FIGURE 4. **Knockdown of Pin1 does not have a significant effect on TGF-β-induced growth-inhibitory effects.** *A*, knockdown of Pin1 does not have a significant effect on TGF-β-induced growth-inhibitory effects. Pin1 knockdown HaCaT cells and the scrambled control HaCaT cells were treated with or without TGF-β at various concentrations and then subjected to [^{3}H]thymidine incorporation assay. The results represent the average of three independent experiments. *B*, knockdown of Pin1 does not have a significant effect on several TGF-β/Smad target genes. Pin1 knockdown HaCaT cells and the scrambled control HaCaT cells were treated with or without TGF-β for 8 h. The expression levels of Pin1 and several TGF-β/Smad target genes were analyzed by Northern blot analysis as indicated. GAPDH expression levels were also analyzed as a loading control. *C*, the mRNA levels of p15, p21, Smad7, JunB, PAI-1, Bcl-2, and Bub1 in B were quantified by densitometer and normalized to GAPDH mRNA levels. The *bar graphs* represent the average of results from 2 μg of poly(A)$^+$ RNA and 4 μg of poly(A)$^+$ RNA.

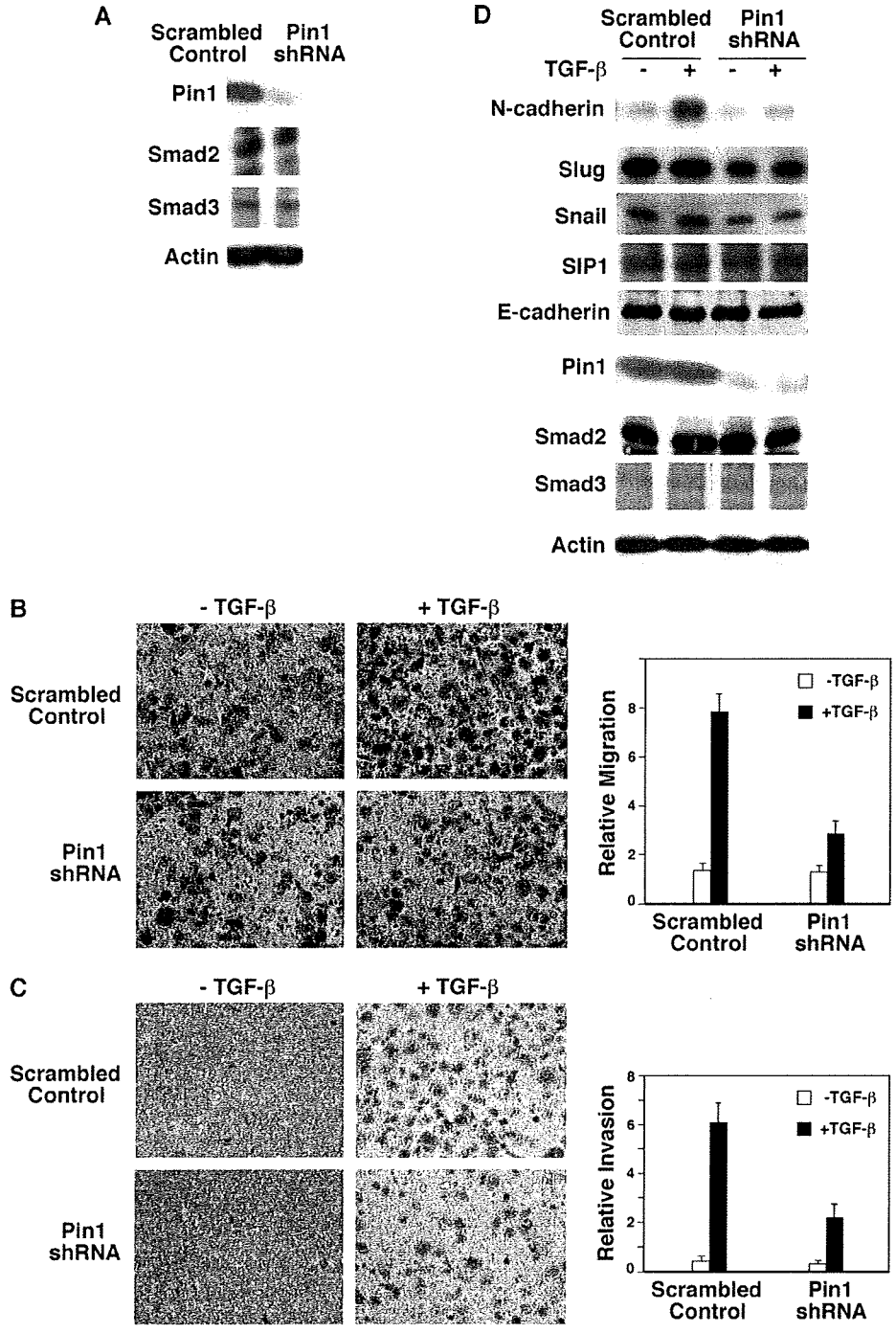

FIGURE 5. **Knockdown of Pin1 significantly reduces TGF-β-induced migration and invasion.** *A*, knockdown of Pin1 has little effect on Smad2/3 levels in the PC3 prostate cancer cells. Stable PC3 prostate cancer cell lines with the shRNA targeting Pin1 or the scrambled control were generated. The cell lysates were analyzed for expression levels of Pin1, Smad2, and Smad3. Actin levels were also analyzed as a loading control. *B*, knockdown of Pin1 significantly reduces TGF-β-induced migration of prostate cancer cells. The Pin1 knockdown PC3 cells and the scrambled control PC3 cells were subjected to the migration assay in the absence or presence of TGF-β. Representative photos of migrated cells were shown. The results from four independent experiments were plotted. *C*, knockdown of Pin1 significantly reduces TGF-β-induced invasion of prostate cancer cells. The Pin1 knockdown PC3 cells and the scrambled control PC3 cells were subjected to the invasion assay in the absence or presence of TGF-β. Representative photos of the invasion assay were shown. The results from four independent experiments were plotted. *D*, knockdown of Pin1 significantly reduces TGF-β induction of N-cadherin expression. The Pin1 knockdown PC3 cells and the scrambled control PC3 cells were treated with or without TGF-β. The cell lysates were analyzed by immunoblot with antibodies against N-cadherin, Slug, Snail, SIP1, E-cadherin, Pin1, Smad2, Smad3, and actin.

TGF-β/Smad3 in hepatocytes (70). As shown in Fig. 4, *B* and *C*, the Bcl2 levels are little affected by TGF-β treatment in the control HaCaT or Pin1 knockdown HaCaT cells, and the Bcl2 levels are very similar between the control cells and the Pin1 knockdown cells. Our previous unpublished results from a subtractive screen suggested that the expression level of Bub1, which regulates the spindle checkpoint function, was slightly reduced in response to TGF-β. We therefore also analyzed Bub1 in the Northern blot analysis. As shown in Fig. 4, *B* and *C*, the expression of Bub1 was slightly reduced in response to TGF-β in both the control cells and the Pin1 knockdown cells. The Bub1 levels at the basal state as well as after TGF-β treatment were modestly reduced in the Pin1 knockdown cells compared with the control cells. The GAPDH levels were also analyzed as a loading control (Fig. 4*B*). Taken together, the results in Fig. 4, *B* and *C*, support the notion that Pin1 does not have a significant effect on TGF-β-mediated growth-inhibitory responses.

Pin1 Promotes TGF-β-mediated Migration and Invasion—Pin1 expression is highly elevated in many cancers (39–51). Based on this notion, we next sought the possible role of Pin1 in TGF-β signaling in cancer cells. TGF-β often promotes cancer cell migration and invasion. We transduced human PC3 prostate cancer cell line with the same shRNA against Pin1 or the scrambled control as used for HaCaT cells. As shown in Fig. 5*A*, Pin1 was also effectively depleted in PC3 cells. Pin1 depletion had little effect on the Smad2 or Smad3 protein levels (Fig. 5*A*). TGF-β-mediated growth-inhibitory response was lost in this cell line (data not shown). On the other hand, TGF-β treatment of the scrambled control PC3 cells greatly stimulated their motility as analyzed in the migration assay (Fig. 5*B*). In the same assay, however, the TGF-β induction of cell motility was significantly reduced when Pin1 was depleted (Fig. 5*B*). Similarly, the

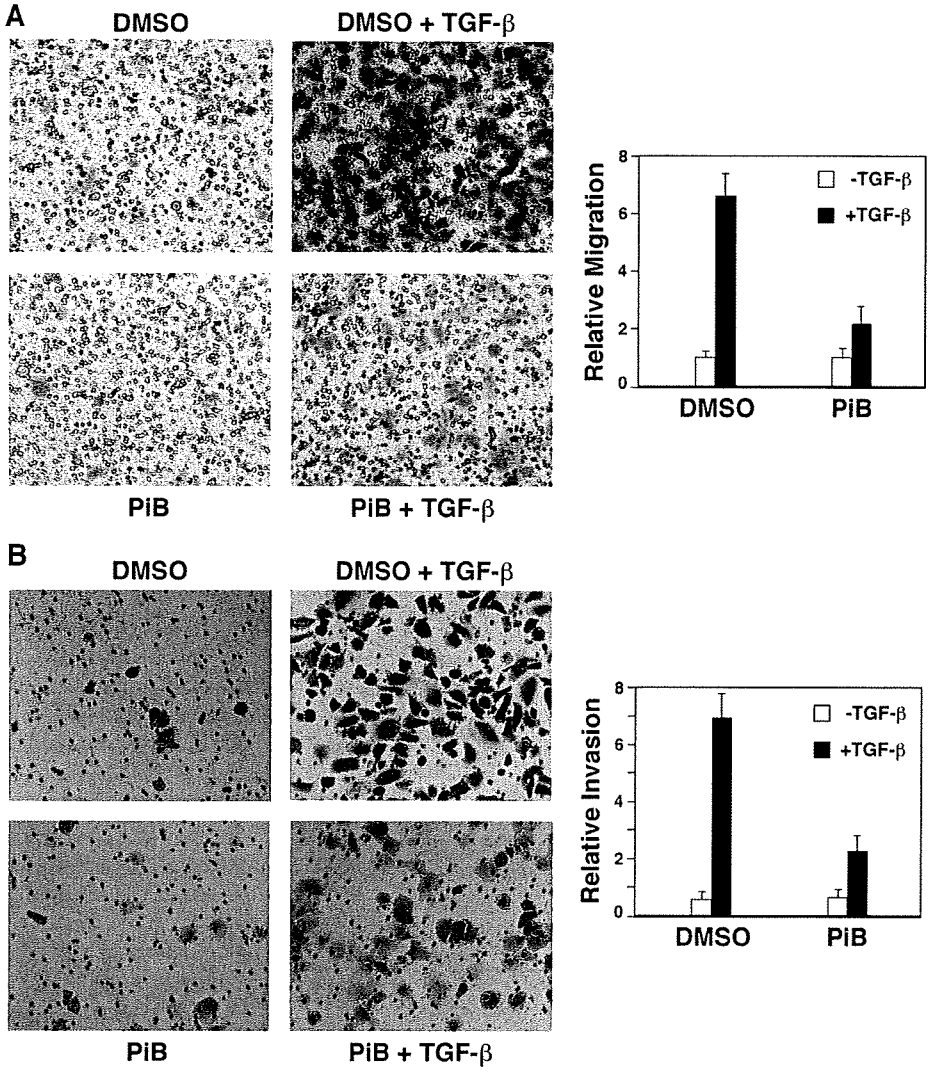

FIGURE 6. **The catalytic activity of Pin1 is necessary for TGF-β-induced migration and invasion.** *A*, the catalytic activity of Pin1 is necessary for TGF-β-induced migration. PC3 cells were subjected to the migration assay in the presence of 1 μM Pin1 inhibitor PiB or the vehicle DMSO control. Cells were treated with or without TGF-β. Representative photos of migrated cells were shown. The results from four independent experiments were plotted. *B*, catalytic activity of Pin1 is necessary for TGF-β-induced invasion. PC3 cells were subjected to the invasion assay in the presence of 1 μM PiB or the vehicle DMSO control. Cells were treated with or without TGF-β. Representative photos of the invasion assay are shown. The results from four independent experiments are plotted.

TGF-β-induced invasion was also significantly reduced in the Pin1 knockdown cells compared with the scrambled control cells (Fig. 5*C*). Thus, Pin1 promotes TGF-β-mediated migratory and invasive responses in the prostate cancer cells. Similar results were also obtained in the MDA-MB-231 breast cancer cells (data not shown). Concomitant with the TGF-β-stimulated migratory and invasive responses in the control PC3 cells, N-cadherin, an important factor for cell migration and invasion (71–77), was up-regulated by TGF-β (Fig. 5*D*). In the Pin1 depleted cells, this up-regulation was greatly reduced (Fig. 5*D*). Thus, the significantly diminished TGF-β-induced cell migration and invasion in the Pin1 knockdown cells was correlated with the greatly reduced expression of N-cadherin.

We also analyzed whether knockdown of Pin1 affects the expression levels of several epithelial mesenchymal transition-related proteins, including Slug, Snail, SIP, and E-cadherin (78–80). As shown in Fig. 5*D*, the expression of Slug and Snail was slightly increased in the presence of TGF-β. Pin1 knockdown reduced the expression of Slug and Snail. However, this effect was not dependent on TGF-β. The expression of SIP1 was slightly increased in the presence of TGF-β (Fig. 5*D*); knockdown of Pin1 had no effect on SIP1 levels in the absence or presence of TGF-β (Fig. 5*D*). The expression of E-cadherin was slightly reduced in the presence of TGF-β (Fig. 5*D*); depletion of Pin1 had no effect on E-cadherin levels in the absence or presence of TGF-β (Fig. 5*D*). These results suggest that these four proteins may not be responsible for the effect of Pin1 in TGF-β-induced migration and invasion.

The Catalytic Activity of Pin1 Is Necessary for TGF-β-induced Migration and Invasion—We next analyzed whether the peptidyl-prolyl cis/trans isomerase activity of Pin1 is necessary for TGF-β-mediated migration and invasion. PiB is a small molecule chemical inhibitor that potently and selectively inhibits Pin1/Par14 isomerase activity through competitively binding to the active site (81–83). PC3 cell migration and invasion assays were performed in the presence of 1 μM PiB or in the presence of the vehicle DMSO, which was used to dissolve PiB. Cells were treated with or without TGF-β. As shown in Fig. 6*A*, PiB significantly inhibited TGF-β-induced migration. Similarly, PiB also significantly inhibited TGF-β-mediated invasion (Fig. 6*B*). Thus, we conclude that the catalytic activity of Pin1 is necessary for its effect in TGF-β-induced migration and invasion.

DISCUSSION

Pin1 is a peptidyl-prolyl cis/trans isomerase that recognizes a small subset of the phosphorylated serine/threonine-proline motifs (39–41). We show in this report that Pin1 binds to Smad2/3 in response to TGF-β. Depletion of Pin1 does not have a significant effect on the Smad2/3 levels as analyzed in the human HaCaT keratinocytes and the human PC3 prostate cancer cells. We further show that the phosphorylated Thr-179-proline motif in the Smad3 linker region is the major binding site for Pin1 after TGF-β treatment and suggest that C-tail

phosphorylation is necessary for association with Pin1. Pin1 binding does not have a significant effect on the phosphorylation levels of Thr-179 or the other sites in the linker region of Smad3 in response to TGF-β. Depletion of Pin1 does not have a significant effect on the TGF-β-induced growth-inhibitory responses. In contrast, depletion of Pin1 markedly reduces TGF-β-induced prostate cancer cell migration and invasion. Similar results were also obtained in the MDA-MB-231 breast cancer cells (data not shown). We conclude that Pin1 promotes TGF-β-mediated migration and invasion.

A recent study by Nakano *et al.* (53) reported that Pin1 enhances Smurf2 interaction with Smad2/3 and leads to decreased levels of Smad2/3. This study showed that knockdown of Pin1 increased Smad2/3 protein levels in the MDA-MB-231 breast cancer cell line (53). Overall, the effect of Pin1 on Smad2/3 protein levels was relatively modest, as quantified in this study. We detected little difference in the Smad2/3 levels in the HaCaT keratinocytes and the PC3 prostate cancer cells when Pin1 was very effectively depleted. One possibility is that the relatively modest Pin1- and Smurf2-dependent degradation of Smad2/3 is cell type-dependent. Previous studies have shown that although Smurf2 binds to Smad3, it does not degrade Smad3 (84, 85). These observations are consistent with the idea of cell-type specificity.

We have shown in this study that Smad2/3 interaction with Pin1 is specific in response to TGF-β. Although EGF induces phosphorylation of the same linker sites as TGF-β to a similar extent, EGF has little effect in inducing Pin1 interaction with Smad2/3. Analysis of the Smad3 mutant at the C-tail phosphorylation sites suggests that the C-tail phosphorylation is necessary for Pin1 binding. The study by Nakano *et al.* (53) showed that a constitutively activated Ras, which leads to Smad2/3 phosphorylation in the linker region, can also induce Smad2/3 binding to Pin1. In addition to activating ERK, which phosphorylates Smad2/3 in the linker region, Ras may have other functions in terms of regulating Smad2/3 phosphorylation. A previous study has shown that Mps1, a dual specificity protein kinase for spindle checkpoint function, can phosphorylate Smad2/3 at the C-tail SSXS motif independent of TGF-β signaling (86). Interestingly, a study showed that constitutively activated B-Raf increased Mps1 protein level and activity (87). Thus, it is possible that the constitutively activated Ras can increase the Mps1 activity, leading to the C-tail phosphorylation of Smad2/3. Both the C-tail and linker phosphorylated Smad2/3 then interact with Pin1. In any case, Pin1 binds to Smad2/3 to a much greater extent in response to TGF-β than in response to the activated Ras (53), indicating the importance of TGF-β in regulating the interaction between Smad2/3 and Pin1.

We have shown in this study that the Thr-179 in the Smad3 linker region plays a major role in the interaction with Pin1 in response to TGF-β. When the Thr-179 site was mutated, Smad3 association with Pin1 was dramatically reduced. This result suggests that Pin1 and Smad3 interact at 1:1 ratio. The recent study by Nakano *et al.* (53) showed that mutation of all four sites in the Smad3 linker region was necessary to disrupt Smad3-Pin1 interaction. Careful analysis of their data, taken into the consideration of the input protein levels, would also suggest that Thr-179 is the major binding site for Smad3 to interact with Pin1.

We analyzed several TGF-β-mediated responses in our studies. Depletion of Pin1 does not have a significant effect on the TGF-β growth-inhibitory responses. We have also analyzed whether depletion of Pin1 affected TGF-β-induced epithelial mesenchymal transition in the PC3 prostate cancer cells, and our studies suggest that depletion of Pin1 modestly reduced TGF-β-mediated epithelial mesenchymal transition in the PC3 cells (data not shown). Thus, Pin1 has a specific role in promoting migration and invasion in response to TGF-β.

The effect of Pin1 in TGF-β-induced migration and invasion is accompanied with the regulation of the expression of N-cadherin, which plays an important role in migration and invasion (71–77), including in the PC3 prostate cancer cells (75). N-cadherin protein levels are induced by TGF-β treatment. When Pin1 is depleted, the TGF-β induction of N-cadherin is dramatically reduced. Analysis of the N-cadherin promoter sequence *in silico* indicates that it contains a consensus Smad binding element, suggesting that Smad proteins may directly bind to its promoter and regulate its expression. Pin1 can induce conformational changes of a number of its substrates (39–41). This can lead to increased protein stability, decreased protein stability, altered transcriptional activity, or other effects (39–41). The effect of Pin1 on TGF-β/Smad target genes varies. For example, Pin1 essentially has no effect on the p15, p21, and Smad7 levels, has a modest inhibitory effect on JunB, has a modest stimulatory effect on PAI-1, and has a significant stimulatory effect on N-cadherin. Thus, the effect of Pin1 on the TGF-β/Smad target genes appears to depend on the promoter context.

Pin1 is overexpressed in many cancers (39–51). Among 60 different tumor types analyzed, 38 tumor types have Pin1 overexpression in 10% to nearly 100% of the cases analyzed, such as prostate, breast, lung, colon, ovary, cervical, brain tumors, and melanoma (44). Thus, Pin1 overexpression is a specific and prevalent event in human cancers. Previous studies have shown that Pin1 is an excellent prognostic marker in prostate cancer (52), the most common cancer in men in the United States. Patients with higher expression of Pin1 have a significantly higher probability of recurrence than patients with low expression of Pin1. In addition, patients with a high expression of Pin1 have almost four times the risk of having earlier recurrence than those patients with low expression of Pin1. Furthermore, patients with a very high level of Pin1 have more than eight times the risk of having earlier recurrence than the patients with a low level of Pin1 (52). TGF-β promotes cancer progression and metastasis. We have shown in this report that Pin1 mediates TGF-β-induced migration and invasion of prostate cancer cells. Pin1 can also promote migration and invasion at basal state (55). Our findings highlight the importance of Pin1 in cancer progression and metastasis, especially for prostate cancer. Furthermore, our findings highly suggest that Pin1 is an important therapeutic target for prostate cancer, breast cancer, and some other types of cancers.

Acknowledgments—We are very grateful to K. Liang for generous help with this project, to L.-H. Wang and members of his laboratory, especially S.-H. Chan, for assisting the migration and invasion assays and for discussions, to E. B. Leof for the Smad3 C-tail phosphopeptide antibody, and to G. Fan, P. Molli, X. Zheng, C. Chu, I. M. Liu, C. Lu, K.-T. Lin, and C. Gelinas for assistance and helpful discussions.

REFERENCES

1. Roberts, A. B., and Sporn, M. B. (1990) in *Peptide Growth Factors and Their Receptors* (Sporn, M. B., and Roberts, A. B., eds) pp. 419–472, Springer-Verlag, Heidelberg, Germany
2. Massagué, J., Blain, S. W., and Lo, R. S. (2000) *Cell* **103,** 295–309
3. Derynck, R., Akhurst, R. J., and Balmain, A. (2001) *Nat. Genet.* **29,** 117–129
4. Roberts, A. B., and Wakefield, L. M. (2003) *Proc. Natl. Acad. Sci. U.S.A.* **100,** 8621–8623
5. Miyazono, K., Suzuki, H., and Imamura, T. (2003) *Cancer Sci.* **94,** 230–234
6. Levy, L., and Hill, C. S. (2006) *Cytokine Growth Factor Rev.* **17,** 41–58
7. Massagué, J. (2008) *Cell* **134,** 215–230
8. Pardali, E., and ten Dijke, P. (2009) *Front. Biosci.* **14,** 4848–4861
9. Heldin, C. H., Miyazono, K., and ten Dijke, P. (1997) *Nature* **390,** 465–471
10. Shi, Y., and Massagué, J. (2003) *Cell* **113,** 685–700
11. Derynck, R., and Zhang, Y. E. (2003) *Nature* **425,** 577–584
12. Liu, F. (2003) *Front. Biosci.* **8,** s1280–1303
13. ten Dijke, P., and Hill, C. S. (2004) *Trends Biochem. Sci.* **29,** 265–273
14. Feng, X. H., and Derynck, R. (2005) *Annu. Rev. Cell Dev. Biol.* **21,** 659–693
15. de Caestecker, M. P., Parks, W. T., Frank, C. J., Castagnino, P., Bottaro, D. P., Roberts, A. B., and Lechleider, R. J. (1998) *Genes Dev.* **12,** 1587–1592
16. Engel, M. E., McDonnell, M. A., Law, B. K., and Moses, H. L. (1999) *J. Biol. Chem.* **274,** 37413–37420
17. Kretzschmar, M., Doody, J., Timokhina, I., and Massagué, J. (1999) *Genes Dev.* **13,** 804–816
18. Hu, P. P., Shen, X., Huang, D., Liu, Y., Counter, C., and Wang, X. F. (1999) *J. Biol. Chem.* **274,** 35381–35387
19. Lehmann, K., Janda, E., Pierreux, C. E., Rytömaa, M., Schulze, A., McMahon, M., Hill, C. S., Beug, H., and Downward, J. (2000) *Genes Dev.* **14,** 2610–2622
20. Blanchette, F., Rivard, N., Rudd, P., Grondin, F., Attisano, L., and Dubois, C. M. (2001) *J. Biol. Chem.* **276,** 33986–33994
21. Attisano, L., and Wrana, J. L. (2002) *Science* **296,** 1646–1647
22. Grimm, O. H., and Gurdon, J. B. (2002) *Nat. Cell Biol.* **4,** 519–522
23. Funaba, M., Zimmerman, C. M., and Mathews, L. S. (2002) *J. Biol. Chem.* **277,** 41361–41368
24. Massague, J. (2003) *Genes Dev.* **17,** 2993–2997
25. Furukawa, F., Matsuzaki, K., Mori, S., Tahashi, Y., Yoshida, K., Sugano, Y., Yamagata, H., Matsushita, M., Seki, T., Inagaki, Y., Nishizawa, M., Fujisawa, J., and Inoue, K. (2003) *Hepatology* **38,** 879–889
26. Matsuura, I., Denissova, N. G., Wang, G., He, D., Long, J., and Liu, F. (2004) *Nature* **430,** 226–231
27. Liu, F., and Matsuura, I. (2005) *Cell Cycle* **4,** 63–66
28. Liu, F. (2006) *Cytokine Growth Factor Rev.* **17,** 9–17
29. Matsuura, I., Wang, G., He, D., and Liu, F. (2005) *Biochemistry* **44,** 12546–12553
30. Mori, S., Matsuzaki, K., Yoshida, K., Furukawa, F., Tahashi, Y., Yamagata, H., Sekimoto, G., Seki, T., Matsui, H., Nishizawa, M., Fujisawa, J., and Okazaki, K. (2004) *Oncogene* **23,** 7416–7429
31. Yamagata, H., Matsuzaki, K., Mori, S., Yoshida, K., Tahashi, Y., Furukawa, F., Sekimoto, G., Watanabe, T., Uemura, Y., Sakaida, N., Yoshioka, K., Kamiyama, Y., Seki, T., and Okazaki, K. (2005) *Cancer Res.* **65,** 157–165
32. Kamaraju, A. K., and Roberts, A. B. (2005) *J. Biol. Chem.* **280,** 1024–1036
33. Javelaud, D., and Mauviel, A. (2005) *Oncogene* **24,** 5742–5750
34. Sapkota, G., Alarcón, C., Spagnoli, F. M., Brivanlou, A. H., and Massagué, J. (2007) *Mol. Cell* **25,** 441–454
35. Guo, X., Ramirez, A., Waddell, D. S., Li, Z., Liu, X., and Wang, X. F. (2008) *Genes Dev.* **22,** 106–120
36. Wang, G., Matsuura, I., He, D., and Liu, F. (2009) *J. Biol. Chem.* **284,** 9663–9673
37. Millet, C., Yamashita, M., Heller, M., Yu, L. R., Veenstra, T. D., and Zhang, Y. E. (2009) *J. Biol. Chem.* **284,** 19808–19816
38. Matsuzaki, K., Kitano, C., Murata, M., Sekimoto, G., Yoshida, K., Uemura, Y., Seki, T., Taketani, S., Fujisawa, J., and Okazaki, K. (2009) *Cancer Res.* **69,** 5321–5330
39. Lu, K. P., and Zhou, X. Z. (2007) *Nat. Rev. Mol. Cell Biol.* **8,** 904–916
40. Yeh, E. S., and Means, A. R. (2007) *Nat. Rev. Cancer.* **7,** 381–388
41. Takahashi, K., Uchida, C., Shin, R. W., Shimazaki, K., and Uchida, T. (2008) *Cell. Mol. Life Sci.* **65,** 359–375
42. Wulf, G. M., Ryo, A., Wulf, G. G., Lee, S. W., Niu, T., Petkova, V., and Lu, K. P. (2001) *EMBO J.* **20,** 3459–3472
43. Ryo, A., Nakamura, M., Wulf, G., Liou, Y. C., and Lu, K. P. (2001) *Nat. Cell Biol.* **3,** 793–801
44. Bao, L., Kimzey, A., Sauter, G., Sowadski, J. M., Lu, K. P., and Wang, D. G. (2004) *Am. J. Pathol.* **164,** 1727–1737
45. He, J., Zhou, F., Shao, K., Hang, J., Wang, H., Rayburn, E., Xiao, Z. X., Lee, S. W., Xue, Q., Feng, X. L., Shi, S. S., Zhang, C. Y., and Zhang, S. (2007) *Lung Cancer* **56,** 51–58
46. Kim, C. J., Cho, Y. G., Park, Y. G., Nam, S. W., Kim, S. Y., Lee, S. H., Yoo, N. J., Lee, J. Y., and Park, W. S. (2005) *World J. Gastroenterol.* **11,** 5006–5009
47. Pang, R., Yuen, J., Yuen, M. F., Lai, C. L., Lee, T. K., Man, K., Poon, R. T., Fan, S. T., Wong, C. M., Ng, I. O., Kwong, Y. L., and Tse, E. (2004) *Oncogene* **23,** 4182–4186
48. Pang, R. W., Lee, T. K., Man, K., Poon, R. T., Fan, S. T., Kwong, Y. L., and Tse, E. (2006) *J. Pathol.* **210,** 19–25
49. Chen, S. Y., Wulf, G., Zhou, X. Z., Rubin, M. A., Lu, K. P., and Balk, S. P. (2006) *Mol. Cell. Biol.* **26,** 929–939
50. Lam, P. B., Burga, L. N., Wu, B. P., Hofstatter, E. W., Lu, K. P., and Wulf, G. M. (2008) *Mol. Cancer* **7,** 91
51. Fan, G., Fan, Y., Gupta, N., Matsuura, I., Liu, F., Zhou, X. Z., Lu, K. P., and Gélinas, C. (2009) *Cancer Res.* **69,** 4589–4597
52. Ayala, G., Wang, D., Wulf, G., Frolov, A., Li, R., Sowadski, J., Wheeler, T. M., Lu, K. P., and Bao, L. (2003) *Cancer Res.* **63,** 6244–6251
53. Nakano, A., Koinuma, D., Miyazawa, K., Uchida, T., Saitoh, M., Kawabata, M., Hanai, J., Akiyama, H., Abe, M., Miyazono, K., Matsumoto, T., and Imamura, T. (2009) *J. Biol. Chem.* **284,** 6109–6115
54. Yaffe, M. B., Schutkowski, M., Shen, M., Zhou, X. Z., Stukenberg, P. T., Rahfeld, J. U., Xu, J., Kuang, J., Kirschner, M. W., Fischer, G., Cantley, L. C., and Lu, K. P. (1997) *Science* **278,** 1957–1960
55. Ryo, A., Uemura, H., Ishiguro, H., Saitoh, T., Yamaguchi, A., Perrem, K., Kubota, Y., Lu, K. P., and Aoki, I. (2005) *Clin. Cancer Res.* **11,** 7523–7531
56. Denissova, N. G., Pouponnot, C., Long, J., He, D., and Liu, F. (2000) *Proc. Natl. Acad. Sci. U.S.A.* **97,** 6397–6402
57. Sachdev, P., Zeng, L., and Wang, L. H. (2002) *J. Biol. Chem.* **277,** 17638–17648
58. Cheng, G. Z., Chan, J., Wang, Q., Zhang, W., Sun, C. D., and Wang, L. H. (2007) *Cancer Res.* **67,** 1979–1987
59. Lu, K. P., Hanes, S. D., and Hunter, T. (1996) *Nature* **380,** 544–547
60. Hannon, G. J., and Beach, D. (1994) *Nature* **371,** 257–261
61. Datto, M. B., Li, Y., Panus, J. F., Howe, D. J., Xiong, Y., and Wang, X. F. (1995) *Proc. Natl. Acad. Sci. U.S.A.* **92,** 5545–5549
62. Feng, X. H., Lin, X., and Derynck, R. (2000) *EMBO J.* **19,** 5178–5193
63. Moustakas, A., and Kardassis, D. (1998) *Proc. Natl. Acad. Sci. U.S.A.* **95,** 6733–6738
64. Pardali, K., Kurisaki, A., Morén, A., ten Dijke, P., Kardassis, D., and Moustakas, A. (2000) *J. Biol. Chem.* **275,** 29244–29256
65. Seoane, J., Le, H. V., Shen, L., Anderson, S. A., and Massagué, J. (2004) *Cell* **117,** 211–223
66. Nagarajan, R. P., Zhang, J., Li, W., and Chen, Y. (1999) *J. Biol. Chem.* **274,** 33412–33418
67. Jonk, L. J., Itoh, S., Heldin, C. H., ten Dijke, P., and Kruijer, W. (1998) *J. Biol. Chem.* **273,** 21145–21152
68. López-Rovira, T., Chalaux, E., Rosa, J. L., Bartrons, R., and Ventura, F. (2000) *J. Biol. Chem.* **275,** 28937–28946
69. Dennler, S., Itoh, S., Vivien, D., ten Dijke, P., Huet, S., and Gauthier, J. M. (1998) *EMBO J.* **17,** 3091–3100
70. Yang, Y. A., Zhang, G. M., Feigenbaum, L., and Zhang, Y. E. (2006) *Cancer Cell* **9,** 445–457
71. Behrens, J. (1993) *Breast Cancer Res. Treat.* **24,** 175–184
72. Gumbiner, B. M. (1996) *Cell* **84,** 345–357
73. Price, J. T., Bonovich, M. T., and Kohn, E. C. (1997) *Crit. Rev. Biochem. Mol. Biol.* **32,** 175–253
74. Derycke, L. D., and Bracke, M. E. (2004) *Int. J. Dev. Biol.* **48,** 463–476
75. Alexander, N. R., Tran, N. L., Rekapally, H., Summers, C. E., Glackin, C., and Heimark, R. L. (2006) *Cancer Res.* **66,** 3365–3369
76. Mariotti, A., Perotti, A., Sessa, C., and Rüegg, C. (2007) *Expert Opin. In-*

vestig. Drugs **16,** 451–465
77. Jin, C., Yang, Y. A., Anver, M. R., Morris, N., Wang, X., and Zhang, Y. E. (2009) *Cancer Res.* **69,** 735–740
78. Miyazono, K. (2009) *Proc. Jpn. Acad. Ser. B Phys. Biol. Sci.* **85,** 314–323
79. Xu, J., Lamouille, S., and Derynck, R. (2009) *Cell Res.* **19,** 156–172
80. Heldin, C. H., Landström, M., and Moustakas, A. (2009) *Curr. Opin. Cell Biol.* **21,** 166–176
81. Uchida, T., Takamiya, M., Takahashi, M., Miyashita, H., Ikeda, H., Terada, T., Matsuo, Y., Shirouzu, M., Yokoyama, S., Fujimori, F., and Hunter, T. (2003) *Chem. Biol.* **10,** 15–24
82. Rustighi, A., Tiberi, L., Soldano, A., Napoli, M., Nuciforo, P., Rosato, A., Kaplan, F., Capobianco, A., Pece, S., Di Fiore, P. P., and Del Sal, G. (2009) *Nat. Cell Biol.* **11,** 133–142
83. Gianni', M., Boldetti, A., Guarnaccia, V., Rambaldi, A., Parrella, E., Raska, I., Jr., Rochette-Egly, C., Del Sal, G., Rustighi, A., Terao, M., and Garattini, E. (2009) *Cancer Res.* **69,** 1016–1026
84. Lin, X., Liang, M., and Feng, X. H. (2000) *J. Biol. Chem.* **275,** 36818–36822
85. Zhang, Y., Chang, C., Gehling, D. J., Hemmati-Brivanlou, A., and Derynck, R. (2001) *Proc. Natl. Acad. Sci. U.S.A.* **98,** 974–979
86. Zhu, S., Wang, W., Clarke, D. C., and Liu, X. (2007) *J. Biol. Chem.* **282,** 18327–18338
87. Cui, Y., and Guadagno, T. M. (2008) *Oncogene* **27,** 3122–3133

THE JOURNAL OF BIOLOGICAL CHEMISTRY VOL. 284, NO. 42, pp. 28642–28649, October 16, 2009

Paraquat Toxicity Induced by Voltage-dependent Anion Channel 1 Acts as an NADH-dependent Oxidoreductase*[S]

Received for publication, June 12, 2009, and in revised form, August 7, 2009 Published, JBC Papers in Press, August 28, 2009, DOI 10.1074/jbc.M109.033431

Hiroki Shimada[‡1], Kei-Ichi Hirai[§], Eriko Simamura[‡], Toshihisa Hatta[‡], Hiroki Iwakiri[¶], Keiji Mizuki[¶], Taizo Hatta[¶], Tatsuya Sawasaki[‖], Satoko Matsunaga[‖], Yaeta Endo[‖**], and Shigeomi Shimizu[‡‡]**

*From [‡]Molecular and Cell Structural Science, Kanazawa Medical University, Uchinada, Ishikawa 920-0293, the [§]Niwa Institute for Immunology, Tosashimizu, Kochi 787-0306, the [¶]Department of Nanoscience, Sojo University, Ikeda, Kumamoto 860-0082, the [‖]Cell-free Science and Technology Research Center and the Venture Business Laboratory, Ehime University, Matsuyama, Ehime 790-8577, the **RIKEN Genomic Sciences Center, Tsurumi, Yokohama 230-0045, and the [‡‡]Department of Pathological Cell Biology, Medical Research Institute, Tokyo Medical and Dental University, Yushima, Bunkyo, Tokyo 113-8510, Japan*

Paraquat (PQ), a herbicide used worldwide, causes fatal injury to organs upon high dose ingestion. Treatments for PQ poisoning are unreliable, and numerous deaths have been attributed inappropriate usage of the agent. It is generally speculated that a microsomal drug-metabolizing enzyme system is responsible for PQ toxicity. However, recent studies have demonstrated cytotoxicity via mitochondria, and therefore, the cytotoxic mechanism remains controversial. Here, we demonstrated that mitochondrial NADH-dependent PQ reductase containing a voltage-dependent anion channel 1 (VDAC1) is responsible for PQ cytotoxicity. When mitochondria were incubated with NADH and PQ, superoxide anion (O_2^-) was produced, and the mitochondria ruptured. Outer membrane extract oxidized NADH in a PQ dose-dependent manner, and oxidation was suppressed by VDAC inhibitors. Zymographic analysis revealed the presence of VDAC1 protein in the oxidoreductase, and the direct binding of PQ to VDAC1 was demonstrated using biotinylated PQ. VDAC1-overexpressing cells showed increased O_2^- production and cytotoxicity, both of which were suppressed in VDAC1 knockdown cells. These results indicated that a VDAC1-containing mitochondrial system is involved in PQ poisoning. These insights into the mechanism of PQ poisoning not only demonstrated novel physiological functions of VDAC protein, but they may facilitate the development of new therapeutic approaches.

Paraquat (PQ^{2+}; methyl viologen, 1,1′-dimethyl-4,4′-bipyridinium dichloride) is an effective herbicide used in more than 120 countries (1). Although it is classified as a low hazard compound, PQ is hazardous when used improperly and has been found responsible for thousands of deaths worldwide because of intentional overdose and high levels of occupational and accidental exposure especially in developing countries (1). Direct exposure to PQ causes severe irritation to the eyes and skin, and ingestion of concentrated products may result in fatal injury to lungs because of edema, hemorrhage, and subsequent fibrosis as well as damage to other organs (2). Additionally, PQ has emerged as a risk factor for Parkinson disease (3). The acute toxicity of PQ in mammals is mediated by reactive oxygen species (ROS) produced by a cyclic oxidation-reduction reaction (4). It is generally speculated that NADPH-cytochrome P450 reductase in microsomal drug-metabolizing enzyme systems is responsible for the production of ROS (5). However, we previously observed that the initial ultrastructural alterations associated with PQ exposure occurred only in mitochondria and not in the endoplasmic reticulum in pulmonary cells *in vivo* (6) and *in vitro* (7). In addition, several reports have suggested the cytotoxicity of PQ via mitochondrial dysfunction (8–10). Despite the development of a number of treatments for PQ poisoning, the efficacy and reliability of currently available treatments have remained limited because of an insufficient understanding of PQ cytotoxicity (2).

We recently discovered that active NADH-dependent oxidoreductase located on the mitochondrial outer membrane reduced PQ to a radical form that spontaneously formed superoxide anion (O_2^-) and destroyed mitochondria (11–13). Furthermore, we demonstrated that 1) PQ was initially metabolized to monopyridone in the cytosol and subsequently hydroxylated by the microsomes and 2) the induction of drug-metabolizing enzymes and the administration of a ROS scavenger reduced PQ toxicity in mice (11, 14). These results indicate that the mitochondrial system, not the microsomal system, is responsible for PQ toxicity. We verified that enzymes in the electron transport chain and NADH-cytochrome b_5 reductase, an NADH-dependent oxidoreductase in the outer membrane, were not involved in this reaction (11, 12). A voltage-dependent anion channel (VDAC), an abundant pore-forming protein in the outer membrane, exerts numerous physiological functions as a channel; it regulates both the metabolite flux of mitochondria and transmembrane potential, and plays a role in apoptosis. Recently, it was reported that NADH regulates VDAC func-

* This work was supported by Grants-in-aid for Scientific Research 15591664, 17591899, 19390291, and 21791045 from the Japan Society for the Promotion of Science, Grants for Promoted Research S2003-12, S2004-12, C2007-4, S2007-9, C2008-1, S2008-10, C2009-3, and S2009-10 from Kanazawa Medical University, Grant for Project Research H2009-14 from High-Tech Research Center of Kanazawa Medical University, and in part by The Ministry of Education, Culture, Sports, Science, and Technology, Japan Grant S0801085.

[S] The on-line version of this article (available at http://www.jbc.org) contains supplemental schemes.

[1] To whom correspondence should be addressed. Fax: 81-76-218-8189; E-mail: simada-h@kanazawa-med.ac.jp.

[2] The abbreviations used are: PQ, paraquat; BQ, benzoquinone; DCF, 2′,7′-dichlorofluorescein; DCFH, DCF-diacetate; DIDS, 4,4′-diisothiocyanatostilbene-2,29-disulfic acid; IC_{50}, 50% growth inhibition toxicity; mAb, monoclonal antibody; PTP, permeability transition pore; TBS, Tris-buffered saline; VDAC, voltage-dependent anion channel; ROS, reactive oxygen species; SOD, superoxide dismutase; siRNA, small Interfering RNA.

tion (15), and an isoform of VDAC localized in the plasma membrane possesses NADH-ferricyanide reductase activity (16). Therefore, we attempted to determine whether or not NADH-PQ oxidoreductase on mitochondria is responsible for PQ cytotoxicity and if VDAC participates in this activity.

EXPERIMENTAL PROCEDURES

Cell Line

HeLa cells were provided by RIKEN Cell Bank (Tsukuba, Japan). Cells were cultured in Dulbecco's modified Eagle's medium (Sigma-Aldrich) supplemented with 10% fetal bovine serum at 37 °C in a humidified CO_2 incubator.

Intracellular ROS Production

Mitochondrial superoxide production in HeLa cells was detected using MitoSOX® (Molecular Probes Inc., Eugene, OR), a red fluorescent mitochondrial superoxide indicator, according to the given protocol. Cells were pretreated with 1 mM PQ; Sigma-Aldrich) for 50 min at 37 °C and incubated with 5 μM MitoSOX for 10 min in the dark. The medium was exchanged for fresh medium, and the cells were observed by a fluorescence microscope (Olympus IX70, Olympus Corp., Tokyo, Japan). The effects of benzoquinone (BQ; 0.2 mM, Sigma-Aldrich) were evaluated after 10 min of incubation in BQ-added medium. Intracellular H_2O_2 production in HeLa cells by PQ was detected using 2′,7′-dichlorofluorescein-diacetate (DCFH; Molecular Probes) (17, 18). Briefly, cells were pretreated with 1 mM PQ for 1 h at 37 °C, and then the cells were incubated with 5 μM DCFH for 20 min in the dark. Afterward, the medium was exchanged for fresh medium; fluorescence images that appeared after the formation of 2′,7′-dichlorofluorescein (DCF) were observed by fluorescence microscopy.

Preparation of Mitochondria

Mitochondria were isolated from the livers of male Wistar rats or from HeLa cells by differential centrifugation (11, 12). Mitochondria were suspended in 0.25 M sucrose solution containing 0.05 M Tris-HCl, 20 mM KCl, 2.0 mM $MgCl_2$, and 1.0 mM Na_2HPO_4 (pH 7.4). The mitochondria were starved for 20 min at 37 °C to consume endogenous substrates before use. The Kanazawa Medical University Animal Care and Use Committee approved all studies. All animals were cared for and treated in accordance with the Committee guidelines.

PQ-dependent Hydrogen Peroxide (H_2O_2) Production on Mitochondria

Mitochondria were attached onto a glass-based culture dishes coated with Cell-Tak® (BD Biosciences) (19). The dishes were incubated with 10 mM PQ and 2 mM NADH (Oriental Yeast Co., Ltd., Tokyo, Japan) in the sucrose solution containing 5 μM DCFH, 5 μM rotenone (Sigma-Aldrich), and 1 μM *p*-hydroxymercuribenzoate (Sigma-Aldrich) at 37 °C. Fluorescence images were captured by a digital CCD camera (Pixera Penguin 150 CL, Pixera Corp., Los Gatos, CA) attached to a microscope and were analyzed by Lumina Vision bio-imaging analysis system (Mitani Corp., Fukui, Japan). The fluorescence intensity per 1000 mitochondria was calculated, and the mean value of three areas from each sample was compared. BQ (0.3 mM), anti-VDAC1 monoclonal antibody (mAb; anti-porin 31 HL mAb, 9 μg/ml; Calbiochem), and 4,4′-diisothiocyanatostilbene-2,29-disulfic acid (DIDS; 100 μM, Sigma-Aldrich) were evaluated by addition to the reaction mixture.

Electron Microscopy

Mitochondria were transferred to a sucrose solution containing 3 mM PQ, 2 mM NADH, 5 μM rotenone, 1 μM *p*-hydroxymercuribenzoate, and the solution was reacted for 30 min at 37 °C (11, 12). Superoxide dismutase (SOD; 3000 units/ml, Sigma-Aldrich) effects were evaluated by the addition of SOD to the reaction mixture. Anti-VDAC1 mAb (3 μg/ml) effects were evaluated by preincubation with the mitochondria for 5 min at 37 °C. The reaction was stopped by the addition of cold buffer. Mitochondria were immediately centrifuged, and the packed sediments were covered with 2% glutaraldehyde in phosphate-buffered saline and fixed for 1 h. The fixed clots were prepared for electron microscopy (11) and then observed by a transmission electron microscope (JEM-1200EX, JEOL Co. Ltd, Tokyo, Japan). The percentage of intact mitochondria per area was counted, and the mean of three areas was calculated.

Growth Inhibition Assays

Growth inhibition assays were performed by the stepwise addition of PQ, according to the method described by Saotome (20). Subconfluent HeLa cells were harvested by trypsinization and were precultured on 96-well plates (3×10^3 cells per well) for 24 h. Cells were treated with 7–250 μM PQ and were then cultured for 72 h. The effects of Trolox® (a water-soluble analog of vitamin E; 1 mM, Sigma-Aldrich) were evaluated by its addition to the medium. The 50% growth inhibition toxicity (IC_{50}) was estimated at 72 h.

Extraction of NADH-PQ Oxidoreductase from the Outer Membrane

To extract NADH-PQ oxidoreductase, two-step extraction with Triton X-100, deoxycholate followed by SDS/Igepal® CA-630 was performed (21). The outer membranes were isolated from the mitochondria by discontinuous sucrose gradient centrifugation (12). The isolated outer membranes were suspended in 20 mM Tris-HCl buffer (pH 7.6) containing 1% Triton X-100, 1% sodium deoxycholate, and 1 mM EDTA. The suspensions were left to stand on ice for 1 h. Suspensions were then centrifuged at 105,000 × *g* for 60 min. The precipitates were resuspended in a 20 mM Tris buffer with 0.06% SDS and 0.1% Igepal CA-630. The suspensions were left on ice for 1 h. The supernatants were collected by centrifugation at 105,000 × *g*.

Preparation of NADH-PQ Oxidoreductase Fraction

The supernatants were diluted with 20 mM Tris-HCl buffer (pH 8.0) containing 0.03% Triton X-100 and 10% glycerol, and the dilutions were loaded onto an anion exchange column (DEAE MemSep® 1000; Millipore Corp. Billerica, MA). The columns were washed with the Tris buffer, and proteins were eluted using a NaCl gradient. The fractions containing NADH-PQ oxidoreductase were collected from 0.25–0.3 M

NaCl fractions and dialyzed against a 20 mM Tris-HCl buffer (pH 7.6) containing 0.03% Triton X-100 and 10% glycerol.

Assays of NADH-PQ Oxidoreductase Activity

NADH Oxidation—The extracts were incubated with 0.2 mM NADH in Tris-buffered saline (TBS) containing 5 μM rotenone and 1 μM *p*-hydroxymercuribenzoate at 37 °C followed by the addition of 10 mM PQ. Activities were calculated by the first-order velocity of NADH oxidation measured at $\lambda_{340\ nm}$ ($e = 6.3 \times 10^3\ M^{-1}cm^{-1}$).

O_2^- Production—O_2^- production by NADH-PQ oxidoreductase activity was assayed using a Diogenes® luminescence system (National Diagnostics Inc., Atlanta, GA). The extracts were mixed with NADH (0.1 mM), PQ (0.0012–5 mM), and Diogenes (3-fold dilution) in TBS on a 384-well plate. The effects of DIDS (100 μM) and anti-VDAC1 mAb (30 μg/ml) were evaluated by the addition of these reagents to the mixture. The total volume of the reaction mixture was 15 μl. Chemiluminescence produced by superoxide was detected by an Envision® multilabel plate reader (PerkinElmer Life Sciences).

Immunoprecipitation

The extracts were incubated with anti-VDAC1 mAb or normal mouse IgG as a control. After incubation in TBS for 90 min at 4 °C, Protein A slurries (Amersham Biosciences) were added to the solution and gently stirred for 90 min at 4 °C. The suspensions were centrifuged, and the supernatants were obtained for the assay.

Zymography and Western Blot Analysis

The NADH-PQ oxidoreductase fraction was mixed with 0.125 M Tris-HCl buffer (pH 6.8) containing 20% glycerol and 0.02% bromphenol blue (1:1, v/v), and the mixture was loaded on native-polyacrylamide gel (5–10% gradient gel; Funakoshi, Tokyo, Japan). Electrophoresis was performed at 5 mA for 5 h on ice, and the gel was immersed in 20 mM Tris-HCl buffer (pH 7.4) containing 20% glycerol, 0.25 mM nitro blue tetrazolium, 5 μM rotenone, and 1 μM *p*-hydroxymercuribenzoate. The gel was incubated with 2 mM NADH and 10 mM PQ at room temperature for 30 min and washed with TBS, and the active bands were stained by diformazan. The electrophoresed gel was blotted, and detection was performed with anti-VDAC1 mAb. Additionally, the active band was excised and subjected to SDS-PAGE followed by Western blot analysis with anti-VDAC1 mAb.

Synthesis of Biotinylated PQ

The biotinylated paraquat was synthesized in moderate yield by condensation reaction of (+)-biotin and 3-(1′-methyl-4,4′-bipyridinium)propylammonium salt, which was prepared by successive *N*-alkylation of 4,4′-bipyridine with iodomethane and 3-bromopropylamine hydrobromide. See the supplemental methods for detailed procedures.

Plasmid Construction

Human *vdac1* cDNA was isolated as an XhoI fragment by PCR and was subcloned into pUC-CAGGS expression vector (22).

Synthesis of VDAC1 Protein Using a Cell-free Protein Synthesis System

The cDNA of VDAC1 was used. For wheat cell-free protein production of VDAC proteins, the VDAC DNA templates were constructed by "split-primer" PCR (23). The first round of PCR was performed on the cDNA using 10 nM concentrations of each of the following primers: a specific primer (5′-CCACCCACCACCACCAATGGCTGTGCCACCCACGT and AODA2306 primer, 5′-AGCGTCAGACCCCGTAGAAA). Then a second round of PCR was carried out to construct the templates for protein synthesis using a portion (5 μl) of the first PCR mix: 100 nM SPu primer (5′-GCGTAGCATTTAGGTGACACT), 100 nM AODA2303 primer (5′-GTCAGACCCCGTAGAAAAGA), and 1 nM deSP6E02 (5′-GGTGACACTATAGAACTCACCTATCTCTCTACACAAAACATTTCCCTACATACAACTTTCAACTTCCTATTCCACCCACCACCACCAATG). Wheat cell-free protein synthesis of VDAC protein was carried out using a robotic synthesizer (24, 25), GenDecorder1000® (CellFree Sciences, Yokohama, Japan) as described below. First, the transcript was created from each of the DNA templates mentioned above using SP6 RNA polymerase. The synthetic mRNAs were then precipitated with ethanol and collected by centrifugation using a Hitachi R10H rotor. Each mRNA (usually 30–35 μg) was washed and transferred into a translation mixture. The translation reaction was performed in the bilayer mode (26) with slight modifications. The translation mixture that formed the bottom layer consisted of 60 A260 units of wheat germ extract (CellFree Sciences) and 2 μg of creatine kinase (Roche Diagnostics) in 25 μl of SUB-AMIX® (CellFree Sciences). The SUB-AMIX® contained (final concentrations) 30 mM Hepes/KOH at pH 8.0, 1.2 mM ATP, 0.25 mM GTP, 16 mM creatine phosphate, 4 mM dithiothreitol, 0.4 mM spermidine, 0.3 mM concentrations of each of the 20 amino acids, 2.7 mM magnesium acetate, and 100 mM potassium acetate. 125 μl of the SUB-AMIX was placed on the top of the translation mixture, forming the upper layer. After incubation at 26 °C for 17 h, the synthesized proteins were confirmed by SDS-PAGE.

Binding Assay

The synthesized VDAC1 protein was mixed with biotinylated PQ (0–1.0 μM) in TBS containing 10% EZ block (Atto Corp., Tokyo, Japan) for 1 h. The mixtures were added to Nunc Immobilizer® streptavidin plates (Nunc, Roskilde, Denmark), which were incubated for 2 h. The plates were then washed with TBS containing 0.1% Tween 20 (TTBS). VDAC1 protein bound to biotinylated PQ was detected by anti-VDAC1 mAb (Calbiochem) followed by the addition of horseradish peroxidase-conjugated second antibody. ECL plus® (GE Healthcare) was used as a substrate of horseradish peroxidase. For NADH binding assay, biotinylated NAD^+ (R&D Systems, Inc., Minneapolis, MN) was mixed with outer membrane extract, and serial dilutions of non-labeled NADH were added for 1 h. The mixtures were incubated with anti-VDAC1 mAb, which was immobilized on Nunc Immobilizer 96-well plates in 10% EZ block (Atto Corp) for 2 h. The plates were washed with TTBS to which ExtrAvidin® peroxidase (Sigma) was added followed by a wash

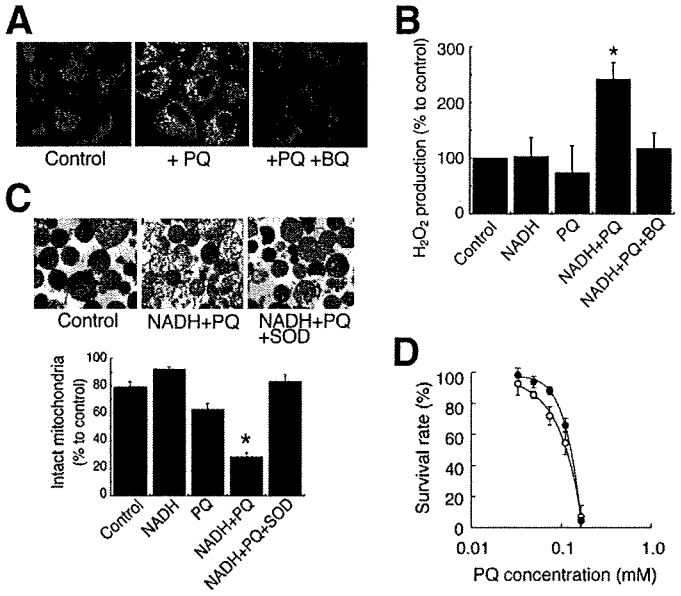

FIGURE 1. **Damage to mitochondria caused by NADH-dependent $O_2^{\cdot-}$ production induced by PQ.** *A*, mitochondrial $O_2^{\cdot-}$ production was visualized by MitoSOX in cells treated with PQ (1 mM) and BQ (0.2 mM). *B*, H_2O_2 production in isolated mitochondria was estimated by DCF florescence method. Mitochondria were incubated with 10 mM PQ, 2 mM NADH, and 0.3 mM BQ (*, $p < 0.01$, *versus* control). *C*, isolated mitochondria were incubated with 3 mM PQ, 2 mM NADH, and the 3000 IU/ml SOD. *Upper panels*, electron micrograph. *Lower graph*, percentages of intact mitochondria (*, $p < 0.001$, *versus* control). *D*, the survival rate of HeLa cells exposed to PQ (*open circle*) and PQ and 1 mM Trolox® (*closed circle*). Each point is the average of two to four experiments. *Error bars* represent S.E.

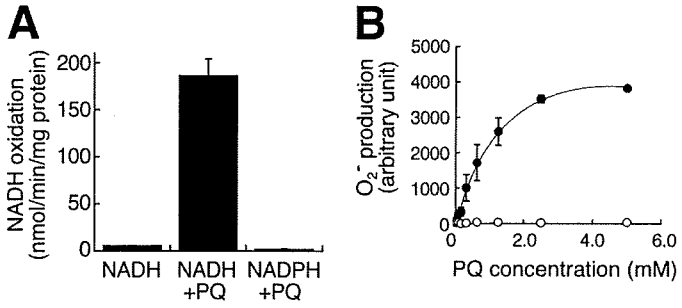

FIGURE 2. **NADH-PQ oxidoreductase activity in the outer membrane extract.** *A*, NADH (0.2 mM) was oxidized by the outer membrane extract in the presence of PQ (5 mM), but NADPH (0.2 mM) was not oxidized. *B*, PQ dose-dependent relationship to $O_2^{\cdot-}$ production activity was observed by co-administration with NADH (0.1 mM) to the outer membrane extract (*closed circle*). In contrast, NADPH (0.1 mM) did not exert any such PQ effects (*open circle*). All *error bars* represent S.D. ($n = 3$).

with TTBS. ECL plus was used for the detection of binding. Immobilized normal mouse IgG was used as a control.

DNA Transfection

HeLa cells were transfected with the VDAC1 plasmid using Effectene® (Qiagen GmbH, Hilden, Germany).

Small Interfering RNA (siRNA) Transfection

HeLa cells were transfected for 72 h with 5 nM control siRNA or Hs_VDAC1_1HP_siRNA (Qiagen) using HiPerFect® transfection reagent (Qiagen).

Statistics

Statistical analyses were conducted using analysis of variance for multiple comparisons and Student's *t* test for comparing two groups.

RESULTS

PQ Produces $O_2^{\cdot-}$ in an NADH-dependent Manner—We first investigated whether PQ produced ROS on mitochondria in HeLa cells. We detected $O_2^{\cdot-}$ on the mitochondria using MitoSOX fluorogenic dye (Fig. 1*A*). Whereas only slight fluorescence was detected on the mitochondria in cells exposed to normal conditions, highly intense levels of fluorescence were observed when the cells were exposed to PQ. Fluorescence was reduced to the control level with the addition of BQ, a scavenger of $O_2^{\cdot-}$. In isolated rat liver mitochondria, we detected the NADH-dependent production of H_2O_2 by PQ using DCFH fluorescent dye (Fig. 1*B*). Although the fluorescence intensity did not change when PQ or NADH alone was added to the isolated mitochondria, the addition of PQ in combination with NADH raised the intensity of fluorescence in the mitochondria. BQ suppressed this augmentation. We also observed that the co-administration of PQ and NADH led to a loss of structural integrity of the isolated mitochondria, and SOD suppressed this damage (Fig. 1*C*). Furthermore, Torolox®, an $O_2^{\cdot-}$ scavenger, significantly increased the survival rates of HeLa cells exposed to PQ ($p < 0.05$, Fig. 1*D*). These results indicated that PQ produced $O_2^{\cdot-}$ in an NADH-dependent manner in mitochondria and damaged mitochondria followed by cell death.

VDAC1 Is Responsible for NDAH-PQ Oxidoreductase Activity—To reveal the components involved in this activity, we performed two-step extraction with Triton X-100, deoxycholate followed by SDS/Igepal CA-630 from the outer membrane and analyzed SDS/Igepal extract. The extract oxidized NADH, but not NADPH, by the addition of PQ (Fig. 2*A*), and $O_2^{\cdot-}$ was produced in a PQ dose-dependent manner (Fig. 2*B*). The NADH oxidation activity was 4.4 times that of the Triton X-100/deoxycholate extract (data not shown). To ascertain whether or not VDAC protein is involved in NADH-PQ oxidoreductase activity, we examined the effects of VDAC inhibitors on this activity (Fig. 3*A*). $O_2^{\cdot-}$ production by the extract from the outer membrane mixed with PQ and NADH was significantly inhibited by DIDS, an anion channel inhibitor, or anti-VDAC1 mAb, but such inhibition was not observed with exposure of the extract to normal mouse IgG. When the extract was immunoprecipitated with anti-VDAC1 mAb, the activity in the supernatant was lower than that observed with the administration of normal IgG (Fig. 3*B*). Furthermore, we confirmed that DIDS and anti-VDAC1 mAb inhibited the production of $O_2^{\cdot-}$ and also inhibited the breakdown of isolated mitochondria exposed to PQ and NADH (Fig. 3, *C* and *D*). These results suggest that VDAC1 is responsible for NADH-PQ oxidoreductase activity.

VDAC1 Is Component of NADH-PQ Oxidoreductase—Because, VDAC1 protein was more highly concentrated in the SDS/Igepal extract than in the Triton X-100/deoxycholate extract (Fig. 4*A*), we investigated whether or not VDAC1 protein is contained in the oxidoreductase. We purified the active fraction from the SDS/Igepal extract using DEAE chromatography and carried out zymography on the fraction by native PAGE in blue tetrazolium solution with PQ and NADH. A

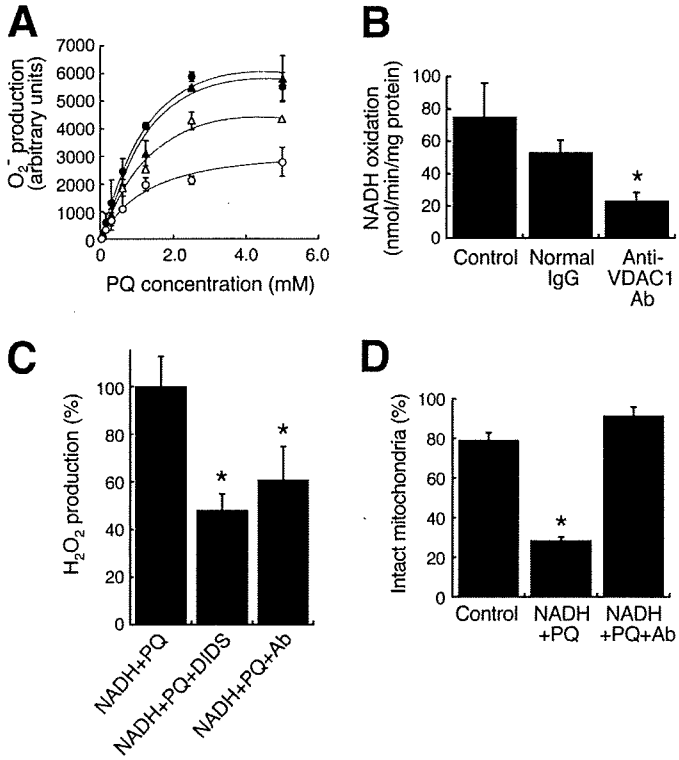

FIGURE 3. **Participation of VDAC1 in the NADH-PQ oxidoreductase activity and mitochondrial damage.** *A*, O_2^- production in the outer membrane extract (*closed circle*) was inhibited by DIDS (100 μM; *open circle*, $p < 0.001$, $n = 3$) and anti-VDAC1 mAb (30 μg/ml; *open triangle*, $p < 0.05$, $n = 3$). *Closed triangle*, treated with normal IgG (30 μg/ml). *Error bars* represent S.D. ($n = 3$). *B*, the extract was immunoprecipitated with anti-VDAC1 mAb or normal IgG, and the NADH-oxidation activity of the supernatants was measured. *Control*, no treatment. *, $p < 0.01$, *versus* control. *Error bars* represent S.D. ($n = 3$). *C*, H_2O_2 production in isolated mitochondria by PQ (10 mM) co-administered with NADH (2 mM) was estimated by DCF florescence method. DIDS (100 μM) and anti-VDAC1 mAb (9 μg/ml) were inhibited H_2O_2 production. *, $p < 0.001$ with respect to the control. Each point is the mean of triplicate experiments. *Error bars* represent S.E. *D*, effects of anti-VDAC1 antibody on the NADH-PQ-dependent breakage of mitochondria were estimated. Isolated mitochondria were ruptured by the co-administration of PQ (3 mM) and NADH (2 mM), whereas the addition of anti-VDAC1 mAb (9 μg/ml) protected the mitochondria from such breakage. *, $p < 0.01$ *versus* the control. Each point is the mean of triplicate experiments. *Error bars* represent S.E.

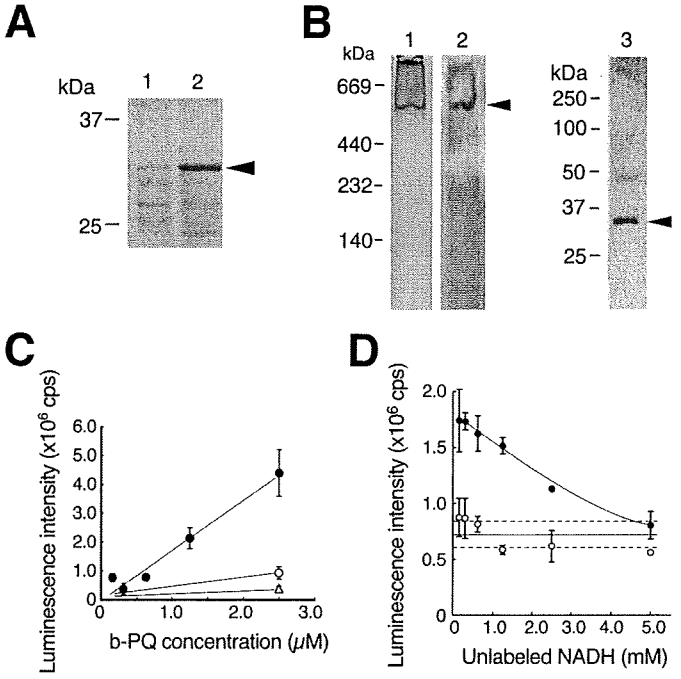

FIGURE 4. **VDAC1 is a component of NADH-PQ oxidoreductase.** *A*, extracts obtained from the mitochondrial outer membrane by treatment with Triton X-100/deoxycholate (*lane 1*) or SDS/ Igepal CA-630 (*lane 2*) were run on SDS-PAGE, and the results were analyzed by Western blotting with anti-VDAC1 mAb. VDAC1 protein was detected by the mAb (*arrowhead*). *B*, DEAE fractions from the extracts containing oxidoreductase activity were examined by zymography with NADH and PQ in blue tetrazolium solution (*lane 1*). The active band was consistent with the anti-VDAC1 mAb-detected band (*lane 2*, *arrowhead*), and this band was excised and subjected to Western blot analysis using anti-VDAC1 mAb (*lane 3*; the *arrowhead* indicates VDAC1 protein). *C*, direct binding to VDAC1 was assayed using biotinylated (*b-*) PQ (*closed circle*) in competition with non-labeled PQ (*open circle*, 25 μM, *open triangle*, 250 μM). *Error bars* represent S.D. ($n = 3$). *D*, assay of NADH binding to the outer membrane extracts was performed. The extracts were trapped by immobilized anti-VDAC1 antibody and incubated with biotinylated NAD^+. Bound biotinylated NAD^+ was reduced by exposure to non-labeled NADH ($p < 0.01$, *closed circles*). When normal IgG was used for trapping, no NADH competition was detected (*open circles*). *Broken lines* represent 95% confidence interval of the control value. *Error bars* represent S.D. ($n = 3$).

major reactive band stained with dark blue diformazan, a form of blue tetrazolium reduced by O_2^-, appeared at 500 kDa (Fig. 4*B*, *lane 1*); this band was recognized using anti-VDAC1 mAb (*lane 2*). Next, the excised band was examined by Western blot analysis with SDS-PAGE using anti-VDAC1 mAb. The antibody recognized a band at 31 kDa, the size of VDAC1 (*lane 3*). Because several proteins were detected in the reactive band by SDS-PAGE followed by silver staining (data not shown), the oxidoreductase may be a complex containing the VDAC1 protein. To confirm the direct interaction of VDAC1 with PQ, we performed a binding assay using recombinant VDAC1 protein and biotinylated PQ (Fig. 4*C*). We detected biotinylated PQ dose-dependently bound to the VDAC1 protein, and excess non-labeled PQ competed for the binding. Next, we examined the interaction of VDAC1 with NADH using biotinylated NAD^+. Whereas the biotinylated NAD^+ was not found to bind to the recombinant VDAC1 protein, which was immobilized by anti-VDAC1 mAb (data not shown), we did detect binding of the biotinylated NAD^+ using the SDS/Igepal extract instead of the VDAC1 protein (Fig. 4*D*). These results were compatible with the absence of NADH-PQ oxidoreductase activity in the recombinant VDAC1 protein or purified VDAC from rat liver mitochondria (data not shown). The present results indicate that VDAC1 is involved in NADH-PQ oxidoreductase activity as a component of the PQ binding site.

VDAC1 Is Responsible for the Cytotoxicity of PQ—Finally, we determined whether the amount of VDAC1 protein in cells affects PQ sensitivity. We obtained stable transfectants of HeLa cells overexpressing VDAC1; these cells had 2.2 times the VDAC1 protein content of control cells (Fig. 5*A*). When treated with PQ, these VDAC1-overexpressing cells showed 2.0 times the intracellular production of H_2O_2 compared with that of control cells (Fig. 5*B*). The IC_{50} of control cells exposed to PQ was 72.3 μM, and this value fell to 30.7 μM in the VDAC1-overexpressing cells (Fig. 5*C*). When HeLa cells were transfected with VDAC1 siRNA, almost no VDAC1 protein was synthesized (Fig. 6*A*). Mitochondria were isolated from these cells, and the NADH-PQ dependent H_2O_2 production was estimated (Fig. 6*B*). The production of H_2O_2 on the mitochondria from knockdown cells was reduced to endogenous levels. The sur-

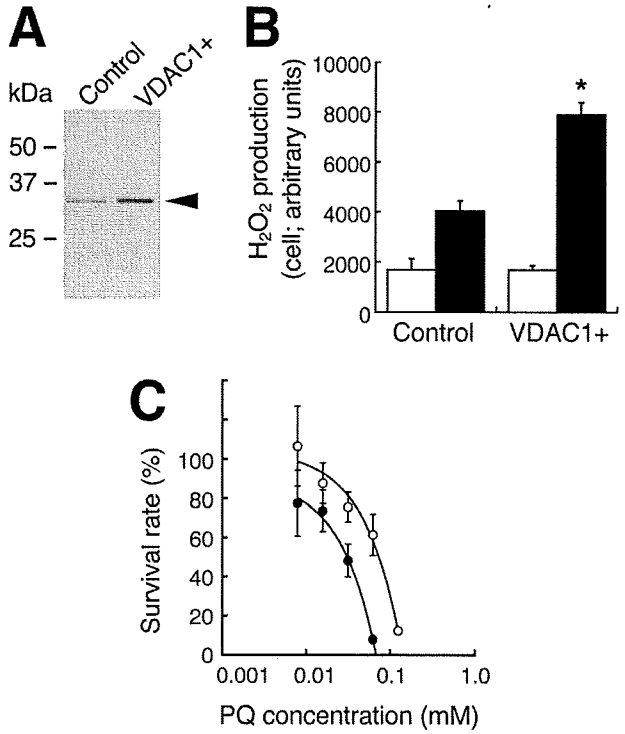

FIGURE 5. **Effects of VDAC1 overexpression on the PQ-dependent H_2O_2 production and the cytotoxicity in HeLa cells.** *A*, lysates from VDAC1-overexpressing cells were subjected to Western blot analysis with anti-VDAC1 mAb. *Control*, cells transfected with empty vector; *VDAC+*, cells transfected with the vector bearing *vdac1* cDNA. *B*, H_2O_2 production by PQ in VDAC1-overexpressing cells (*VDAC1+*) was higher than that of control cells (*, $p < 0.001$). *Light bars*, no treatment; *dark bars*, exposure to 1 mM PQ. *Error bars* represent S.D. ($n = 3$). *C*, the survival rates of VDAC1-overexpressing HeLa cells (*closed circle*) were lower than those of controls (open circle; $p < 0.001$). *Error bars* represent S.E. of triplicate experiments.

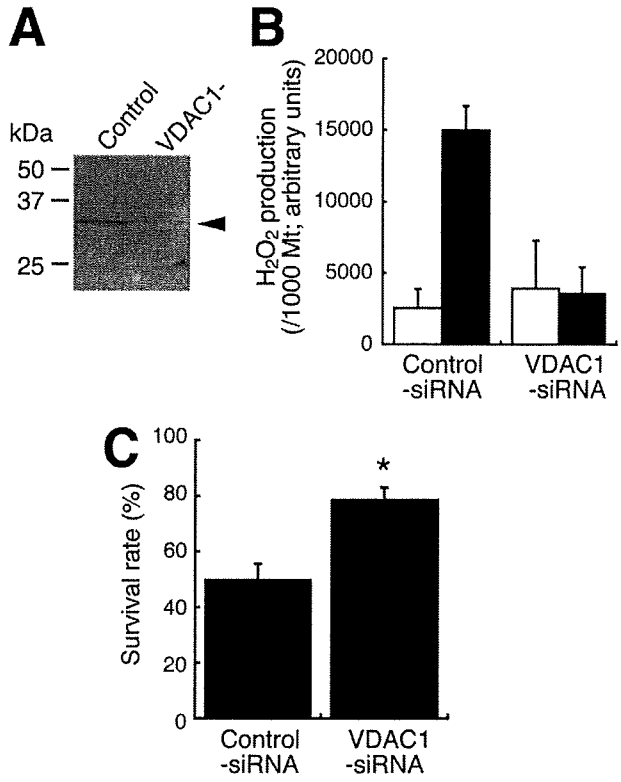

FIGURE 6. **Effects of VDAC1 knockdown on the PQ-dependent H_2O_2 production and the cytotoxicity in HeLa cells.** *A*, lysates from knockdown cells were subjected to Western blot analysis with anti-VDAC1 mAb. *Control*, cells transfected with the control siRNA; *VDAC−*, cells transfected with VDAC1 siRNA. The *arrowheads* indicate VDAC1 protein. *B*, NADH-PQ-dependent H_2O_2 production on mitochondria isolated from VDAC1-knockdown HeLa cells was estimated by DCF assay. *Light bars*, mitochondria incubated with 2 mM NADH only; *dark bars*, mitochondria were incubated with 10 mM PQ and 2 mM NADH. *Error bars* represent S.D. ($n = 3$). *C*, the survival rate of VDAC1-knockdown HeLa cells (VDA1-siRNA) after 24 h of exposure to 222 μM PQ was higher than that of control cells ($p < 0.001$). *Error bars* represent S.E. of triplicate experiments.

vival rate after exposure of the VDAC1 knockdown cells to 222 μM PQ for 24 h was 79% compared with 50% in controls (Fig. 6*C*). These results indicated that VDAC1 is responsible for the cytotoxicity of PQ as an NADH-dependent oxidoreductase.

DISCUSSION

In this study we demonstrate that a mitochondrial system, not a microsomal system, is involved in PQ poisoning; PQ produces O_2^- by NADH-dependent oxidoreductase in the outer membrane of mitochondria and damages mitochondria, leading to cell death. Furthermore, we present that mitochondrial VDAC1 is responsible for this activity as a component of the PQ binding site.

We observed O_2^- production on the mitochondria after administering PQ to cells using MitoSOX, an O_2^--specific fluorescent dye. Additionally, we detected H_2O_2 production on isolated mitochondria in the presence of PQ and NADH using DCFH fluorescent dye, and BQ reduced the level of production. In a previous study we observed that cytochrome *c*, an O_2^- scavenger, diminished H_2O_2 production on mitochondria incubated with PQ and NADH (13). Because O_2^- is immediately (10^5 $M^{-1}s^{-1}$) converted into H_2O_2 in aqueous solution, DCF fluorescence demonstrating H_2O_2 is considered to be equivalent to a demonstration of O_2^- production (13). We also indicated that PQ destroyed isolated mitochondria in the presence of NADH and that SOD suppressed this damage. Furthermore, Trolox® suppressed the toxicity of PQ in cells. We formerly reported that PQ selectively destroyed the mitochondria of pulmonary type II cells and hepatocyte *in vivo* (6, 11) and also destroyed cultured type II cells (7). These results indicate that PQ attacks mitochondria by NADH-dependent O_2^- production in the course of its cytotoxicity.

In an ultrastructural study, we previously observed that NADH-dependent O_2^- production by PQ occurred in the outer membrane of mitochondria (13) and demonstrated that the NADH oxidation activity by PQ in the outer membrane fraction was five times that of the inner membrane fraction (12). O_2 uptake on mitochondria took place with the addition of PQ and NADH (11, 12), and blue PQ radicals formed under anaerobic conditions (11). In the present study we again observed NADH oxidation and PQ radical formation in the outer membrane under anaerobic conditions (data not shown). These results indicated that an NADH-PQ oxidoreductase is localized in the outer membrane. We previously confirmed that NADH-cytochrome b_5 reductase, an outer membrane-localized oxidoreductase, did not participate in the PQ reduction, based on its insensitivity to anti-NADH-cytochrome b_5 reductase antibody and a different sensitivity to *p*-hydroxymercuribenzoate (12). We also reported that rotenone, an inhibitor of complex I in the electron

transport chain, did not inhibit NADH-dependent PQ reduction (11, 12). Intriguingly, we find that VDAC1 is a constituent of the NADH-PQ oxidoreductase. VDAC1 is a small, abundant, pore-forming protein found in the outer membranes of all eukaryotic mitochondria and plays an important role in the passage of adenine nucleotides, Ca^{2+}, and other metabolites through the outer membrane (27). In addition, VDAC1 located at contact sites between the outer and inner membranes forms permeability transition pores (PTPs) with the adenine nucleotide transporter, cyclophilin D, and other proteins (27). It is unknown whether PTP proteins besides VDAC1 participate in the NADH-PQ oxidoreductase activity; thus, it will still be necessary to investigate their involvement with PTP proteins.

Extramitochondrial oxidative stress induces PTP openings via VDAC protein without damage to the inner membrane (27). PQ does not penetrate mitochondrial membrane (28), and O_2^- production by PQ occurs on the outer surface of the outer membrane (13). Furthermore, we demonstrated the binding of PQ to VDAC1 protein by biotinylated PQ and the inhibition of PQ-dependent mitochondrial breakage by anti-VDAC1 mAb. These results indicated that the breakage of mitochondria by PQ occurred through VDAC1. The binding mechanism of PQ, a cation molecule, to VDAC1 remains unknown. It has been reported that NADH increased the voltage dependence of VDAC and reduced the conductance of the outer membrane (29, 30). The ion selectivity of VDAC changed from anions to cations when conductance decreased (31). NADH may, therefore, affect the binding of PQ to VDAC1. Baker *et al.* (16) reported that VDAC1 localized in the plasma membrane functions as NADH-ferricyanide reductase and that VDAC1 has a putative NAD^+ binding motif. Yehezkel *et al.* (32) demonstrated that VDAC purified from rat liver mitochondria had nucleotide binding sites bound to ATP; however, NADH did not bind them. As in a previous study (Hirai *et al.* (11), the change in conformation from the orthodox to the condensed type occurred when NADH was added to starved intact mitochondria. In addition, NADH reduced the permeability of the outer membrane to ADP (15). These results indicated that NADH affects PTP even though NADH does not bind to VDAC1 directly. Although we did not observe the direct binding of NADH to VDAC1 alone, we did observe the binding of biotinylated NAD^+ to the NADH-PQ oxidoreductase concentrated extract, which was trapped by anti-VDAC1 mAb. NADH-PQ oxidoreductase activity was inhibited by DIDS and anti-VDAC1 mAb, but recombinant VDAC1 protein or purified VDAC protein alone had no activity. Therefore, an NADH binding component is expected to be necessary to yield this activity.

Yagoda *et al.* (33) reported that VDAC2 or VDAC3 was implicated in the cytotoxicity of the anti-tumor agent erastin, which was shown to induce oxidative cell death; in particular, VDAC2 was found to bind directly to this agent. We have not yet identified the involvement of VDAC2 or VDAC3 in NADH-PQ oxidoreductase activity. It has been reported that VDAC1 is the most abundantly expressed of the three VDAC isoforms in mammalian mitochondria (34). In addition, we demonstrated a correlation between the production of O_2^- and VDAC1 expression, and we observed defective O_2^- production on the mitochondria isolated from VDAC1 knockdown cells. Therefore, it appears that VDAC1 participates primarily in NADH-PQ oxidoreductase activity. Recently, we found that several furanonaphthoquinones caused mitochondrial damage and the apoptosis of cancer cells by the production of ROS, and other studies revealed that VDAC1 induces ROS production by an NADH-dependent quinone reduction (17, 35). Additionally, we previously demonstrated that menadione, a naphthoquinone, was a substrate of NADH-PQ oxidoreductase (12). These previous and present results taken together suggest that the function of VDAC1 is not only to serve as a channel but also to function as part of an oxidoreductase enzyme.

Until now, management of PQ poisoning has been directed primarily at removing PQ from the gastrointestinal tract by the use of several absorbents (activated charcoal, Fuller's Earth, etc.) and increasing its excretion from the blood by hemoperfusion (2). However, the efficacy of these treatments is poor. Our results indicated that O_2^- production by a VDAC-containing mitochondrial system is responsible for PQ poisoning. DIDS and anti-VDAC1 antibody inhibited NADH-PQ oxidoreductase activity, mitochondrial O_2^- production, and the breakage of mitochondria by PQ. Furthermore, PQ cytotoxicity was suppressed in VDAC1-knockdown cells. These results suggest that specific VDAC inhibitors can be therapeutic agents of PQ poisoning.

Acknowledgment—We are grateful to Mayumi Mitani for secretarial assistance.

REFERENCES

1. Wesseling, C., van Wendel de Joode, B., Ruepert, C., León, C., Monge, P., Hermosillo, H., and Partanen, T. J. (2001) *Int. J. Occup. Environ. Health* **7,** 275–286
2. Dinis-Oliveira, R. J., Duarte, J. A., Sánchez-Navarro, A., Remião, F., Bastos, M. L., and Carvalho, F. (2008) *Crit. Rev. Toxicol.* **38,** 13–71
3. McCormack, A. L., Thiruchelvam, M., Manning-Bog, A. B., Thiffault, C., Langston, J. W., Cory-Slechta, D. A., and Di Monte, D. A. (2002) *Neurobiol. Dis.* **10,** 119–127
4. Baldwin, R. C., Pasi, A., MacGregor, J. T., and Hine, C. H. (1975) *Toxicol. Appl. Pharmacol.* **32,** 298–304
5. Bus, J. S., Cagen, S. Z., Olgaard, M., and Gibson, J. E. (1976) *Toxicol. Appl. Pharmacol.* **35,** 501–513
6. Hirai, K., Witschi, H., and Côté, M. G. (1985) *Exp. Mol. Pathol.* **43,** 242–252
7. Wang, G. Y., Hirai, K., and Shimada, H. (1992) *J. Electron Microsc. (Tokyo)* **41,** 181–184
8. Yang, W., and Tiffany-Castiglioni, E. (2005) *J. Toxicol. Environ. Health A* **68,** 1939–1961
9. St. Clair, D. K., Oberley, T. D., and Ho, Y. S. (1991) *FEBS Lett.* **293,** 199–203
10. Oliver, P. D., and Newsome, D. A. (1992) *Invest. Ophthalmol. Vis. Sci.* **33,** 1909–1918
11. Hirai, K., Ikeda, K., and Wang, G. Y. (1992) *Toxicology* **72,** 1–16
12. Shimada, H., Hirai, K., Simamura, E., and Pan, J. (1998) *Arch Biochem. Biophys* **351,** 75–81
13. Hirai, K. I., Pan, J., Shimada, H., Izuhara, T., Kurihara, T., and Moriguchi, K. (1999) *J. Electron Microsc. (Tokyo)* **48,** 289–296
14. Shimada, H., Furuno, H., Hirai, K., Koyama, J., Ariyama, J., and Simamura, E. (2002) *Arch. Biochem. Biophys.* **402,** 149–157
15. Lee, A. C., Xu, X., and Colombini, M. (1996) *J. Biol. Chem.* **271,** 26724–26731
16. Baker, M. A., Lane, D. J., Ly, J. D., De Pinto, V., and Lawen, A. (2004) *J. Biol. Chem.* **279,** 4811–4819

17. Simamura, E., Hirai, K., Shimada, H., Koyama, J., Niwa, Y., and Shimizu, S. (2006) *Cancer Biol. Ther.* **5,** 1523–1529
18. Ariyama, J., Shimada, H., Aono, M., Tsuchida, H., and Hirai, K. I. (2000) *Intensive Care Med.* **26,** 981–987
19. Nakayama, S., Sakuyama, T., Mitaku, S., and Ohta, Y. (2002) *Biochem. Biophys. Res. Commun.* **290,** 23–28
20. Saotome, K., Morita, H., and Umeda, M. (1989) *Toxicol. In Vitro* **3,** 317–321
21. Teraoka, K., and Matsui, S. (1999) *Nippon Rinsho.* **57,** (suppl.) 784–788
22. Narita, M., Shimizu, S., Ito, T., Chittenden, T., Lutz, R. J., Matsuda, H., and Tsujimoto, Y. (1998) *Proc. Natl. Acad. Sci. U.S.A.* **95,** 14681–14686
23. Sawasaki, T., Ogasawara, T., Morishita, R., and Endo, Y. (2002) *Proc. Natl. Acad. Sci. U.S.A.* **99,** 14652–14657
24. Sawasaki, T., Kamura, N., Matsunaga, S., Saeki, M., Tsuchimochi, M., Morishita, R., and Endo, Y. (2008) *FEBS Lett.* **582,** 221–228
25. Sawasaki, T., Gouda, M. D., Kawasaki, T., Tsuboi, T., Tozawa, Y., Takai, K., and Endo, Y. (2005) *Methods Mol. Biol.* **310,** 131–144
26. Sawasaki, T., Hasegawa, Y., Tsuchimochi, M., Kamura, N., Ogasawara, T., Kuroita, T., and Endo, Y. (2002) *FEBS Lett.* **514,** 102–105
27. Crompton, M. (1999) *Biochem. J.* **341,** 233–249
28. Gage, J. C. (1968) *Biochem. J.* **109,** 757–761
29. Lee, A. C., Zizi, M., and Colombini, M. (1994) *J. Biol. Chem.* **269,** 30974–30980
30. Zizi, M., Byrd, C., Boxus, R., and Colombini, M. (1998) *Biophys. J.* **75,** 704–713
31. Vyssokikh, M., and Brdiczka, D. (2004) *Mol. Cell. Biochem.* **256–257,** 117–126
32. Yehezkel, G., Hadad, N., Zaid, H., Sivan, S., and Shoshan-Barmatz, V. (2006) *J. Biol. Chem.* **281,** 5938–5946
33. Yagoda, N., von Rechenberg, M., Zaganjor, E., Bauer, A. J., Yang, W. S., Fridman, D. J., Wolpaw, A. J., Smukste, I., Peltier, J. M., Boniface, J. J., Smith, R., Lessnick, S. L., Sahasrabudhe, S., and Stockwell, B. R. (2007) *Nature* **447,** 864–868
34. Yamamoto, T., Yamada, A., Watanabe, M., Yoshimura, Y., Yamazaki, N., Yoshimura, Y., Yamauchi, T., Kataoka, M., Nagata, T., Terada, H., and Shinohara, Y. (2006) *J. Proteome Res.* **5,** 3336–3344
35. Simamura, E., Shimada, H., Ishigaki, Y., Hatta, T., Higashi, N., and Hirai, K. I. (2008) *Anat. Sci. Int.* **83,** 261–266

Biosci. Biotechnol. Biochem., 73 (7), 1661–1664, 2009

Note

Construction of a Protein Library of Arabidopsis Transcription Factors Using a Wheat Cell-Free Protein Production System and Its Application for DNA Binding Analysis

Akira NOZAWA,[1,2] Yuko MATSUBARA,[1] Yoshinori TANAKA,[1] Hirotaka TAKAHASHI,[1] Tatsuya AKAGI,[1] Motoaki SEKI,[3] Kazuo SHINOZAKI,[4] Yaeta ENDO,[1,2,†] and Tatsuya SAWASAKI[1,2,†]

[1]*Cell-Free Science and Technology Research Center, and Venture Business Laboratory, Ehime University, 3 Bunkyo-cho, Matsuyama, Ehime 790-8577, Japan*
[2]*Systems and Structural Biology Center, RIKEN, 1-7-22 Suehiro-cho, Tsurumi-ku, Yokohama, Kanagawa 230-0045, Japan*
[3]*Plant Genomic Network Research Team, Plant Functional Genomics Research Group, RIKEN Plant Science Center, 1-7-22 Suehiro-cho, Tsurumi-ku, Yokohama, Kanagawa 230-0045, Japan*
[4]*Gene Discovery Research Team, Gene Discovery Research Group, RIKEN Plant Science Center, 3-1-1 Koyadai, Tsukuba, Ibaraki 305-0074, Japan*

Received January 9, 2009; Accepted February 19, 2009; Online Publication, July 7, 2009
[doi:10.1271/bbb.90026]

We created a protein library consisting of 647 Arabidopsis transcription factors (TFs) using a wheat cell-free system. The quality of proteins in the library was checked by binding assay of bZIP family proteins. Screening of TFs binding to 5′-regulatory regions of *FLC* and *LFY* was conducted using the library, and MYB67 and GBF1 were found to be binding factors.

Key words: Arabidopsis; wheat cell-free protein production system; transcription factor

The completion of entire genome sequences of various organisms has resulted in the identification of large numbers of novel genes.[1)] The challenge ahead is to gain information about the function of these novel genes. Currently, significant effort is devoted to understanding the roles of a gene by analyzing its expression pattern or by analyzing phenotypes of the gene-specific disruption mutant. In addition to this information, biochemical characterization of the protein encoded by the gene is essential for understanding its precise function. However, only slight progress has been made in the large-scale biochemical characterization of proteins, especially at the genome-wide level. To establish a proteomics approach for the characterization of proteins, it is necessary to meet three requirements, availability of i) a wide variety of proteins, ii) sufficient amounts of proteins, and iii) functionally folded proteins.

Transcription factors (TFs) play crucial roles in almost all biological processes. The Arabidopsis genome encodes more than 1,500 transcription factors.[2)] These TFs are classified into various TF families according to the distinct type of DNA binding domains, such as AP2/EREBP, bZIP, HD-ZIP, Myb, MADS, and several classes of zinc finger proteins. TFs control gene expression by binding to specific DNA sequences in the genome. However, the number of TFs whose binding sequences have been confirmed by biochemical analyses is limited, mainly because of the difficulty in obtaining sufficient amounts of purified TF proteins, as they are expressed in small quantities in the cell. Overexpression of recombinant TF proteins in cells is generally difficult because overexpression of TFs often inhibits host cell physiology. Here, we constructed an Arabidopsis TF protein library based on our wheat cell-free protein synthesis system.[3,4)] For evaluation of the library, we performed several biochemical analyses. Our results indicate that the cell-free based Arabidopsis TF protein library is a powerful tool in the large-scale functional analysis of TFs.

Genome analysis revealed at least 1,500 TFs, classifiable into 45 families, in the Arabidopsis genome.[2)] Out of these, cDNA clones of 1,076 TFs were in the RIKEN Arabidopsis full-length (RAFL) clone collection.[5)] *Escherichia coli* cells harboring the cDNA clones were inoculated individually in 96-well plates, and the plates were then incubated for 48 h at 37 °C. DNA templates for transcription were prepared from each *E. coli* clone using the split-primer polymerase chain reaction (PCR) method, as described in our previous reports.[4,6)] Finally, we prepared a total of 705 DNA templates for transcription from the 1,076 RAFL clones. mRNAs were prepared from each amplified DNA template, and the synthesized mRNAs were used for protein synthesis by the bilayer method.[7)] Following this protocol, we created a protein library, AtTF, consisting of 647 synthesized Arabidopsis TFs. The mean values for the amount (concentration) and solubility of all synthesized TFs were 1 μM and 72% respectively (Fig. 1A). The size of each protein synthesized was confirmed by SDS-polyacrylamide gel electrophoresis (PAGE) analysis (data not shown). We did not observe any major difference among the families as far as protein synthesis and solubility were concerned. All the families included both

† To whom correspondence should be addressed. Yaeta ENDO, Fax: +81-89-927-9941; E-mail: yendo@eng.ehime-u.ac.jp; Tatsuya SAWASAKI, Fax: +81-89-927-9941; E-mail: sawasaki@eng.ehime-u.ac.jp

Abbreviations: PAGE, polyacrylamide gel electrophoresis; RAFL, RIKEN Arabidopsis full-length; PCR, polymerase chain reaction; TF, transcription factor; TRR, transcription regulatory region

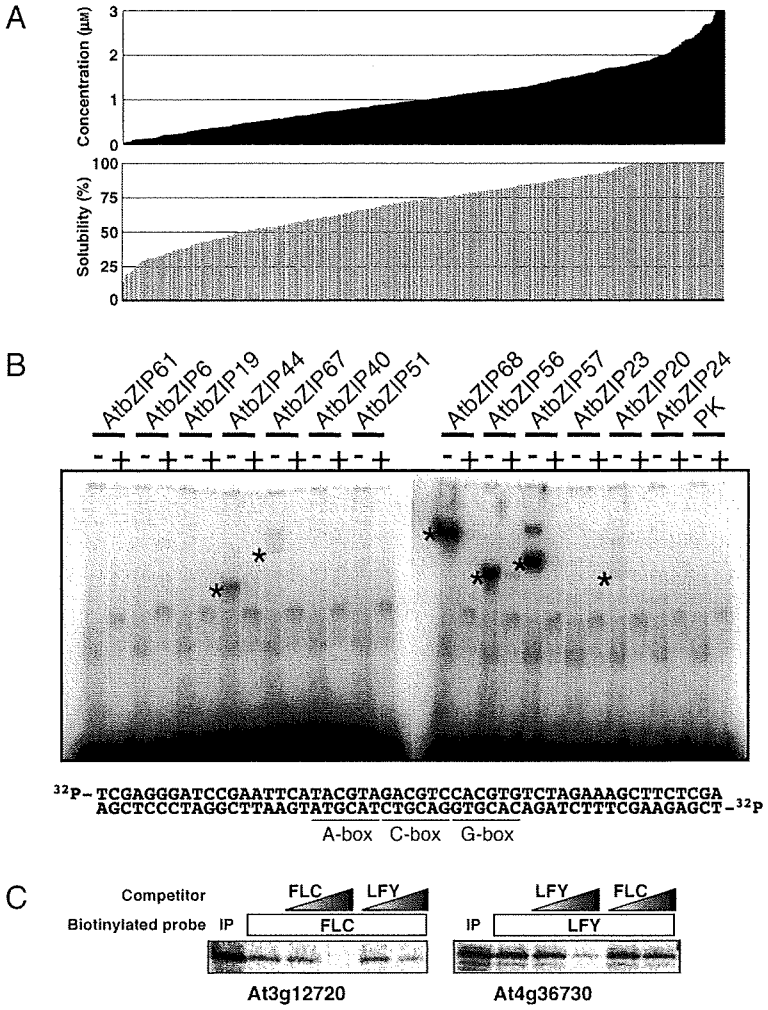

Fig. 1. Construction of a Protein Library of Arabidopsis Transcription Factors and Its Application to DNA Binding Assay.

A, High-throughput production of Arabidopsis TF proteins by the wheat germ cell-free protein synthesis system. Arabidopsis TF proteins (n = 647) were synthesized using the wheat germ cell-free system, as described in the text. The concentration (μM) and solubility of these synthesized TF proteins are shown in separate panels. Results are arrayed so that the value of each parameter increases from left to right in each panel. B, DNA binding analysis of the bZIP proteins. The [^{32}P]-labeled DNA probe (shown at the bottom of the figure) and an indicated bZIP protein were incubated in the presence (+) and the absence (−) of a competitor (10-fold excess of the non-labeled probe). After 30 min of incubation, the samples were subjected to PAGE. Asterisks indicate shifted bands of DNA-protein complex. Lanes of PK show results using a protein kinase, GSK1 (negative control). The nucleotide sequences of the oligonucleotides used as the probe are also shown. The sequences of the A-, C-, and G-boxes are underlined. C, Screening of TF proteins. TF proteins synthesized from cDNA clones (At3g12720 and At4g36730) were incubated with the respective biotinylated promoter probes in the presence and the absence of non-labeled competitor DNA fragment (*FLC* or *LFY*, 5- and 10-fold excess respectively). After 30 min, the samples were pulled down with streptavidin-conjugated magnetic beads, subjected to SDS–PAGE, and detected by autoradiography. IP, proteins inputted to this assay.

poorly-synthesized and well-synthesized TF proteins. There was no TF family from which no members could be synthesized using this cell-free protein synthesis system. These results suggest that our cell-free protein synthesis system can synthesize sufficient quantities of good-quality Arabidopsis TFs for functional analysis.

To determine whether these synthesized TF proteins can be used for functional analysis, we demonstrated two independent DNA binding assays using this protein library. First we examined the DNA binding activity of the bZIP TFs in this library. bZIP TFs have a basic region that binds to the DNA and a leucine zipper dimerization motif.[8] Proteins with bZIP domains are present in all eukaryotes analyzed to date. Some of the bZIP TFs, such as Jun/Fos or CREB, have been extensively studied in animals, and they serve as models for understanding TF-DNA interactions, ternary complex formation, and post-translational modifications.[8] Plant bZIP proteins bind to DNA sequences with an ACGT core, preferentially to A-box (TACGTA), C-box (GACGTC), and G-box (CACGTG).[9] Seventy-five bZIP transcription factors were found in the Arabidopsis genome, and they were classified into 11 groups.[8] In this study, 54 bZIP proteins were synthesized using the cell-free protein synthesis system. Among them, 45 bZIP proteins (60% of the family), concentration of which was approximately 0.4 μM, were used for the binding assay. The DNA-binding ability of each synthesized TF was detected by gel retardation assay using a specific DNA fragment that contained the A-, C-, and G-box. Gel retardation assay was conducted as previously described.[10] DNA-binding ability was confirmed for 19 out of 45 bZIPs proteins. The representative results of gel retardation assay are shown in Fig. 1B. The results of the DNA-binding assay are summarized in Table 1. bZIP proteins belonging to A, C, D, G, H, and S groups were reported to bind DNA sequences with an ACGT core.[8,11–14] Among them, binding of groups A,

Table 1. Results of DNA Binding Assay for the bZIP Family Proteins in Arabidopsis

Name	AGI code	G[a]	Published name	DNA binding	Name	AGI code	G	Published name	DNA binding
AtbZIP40	At1g03970	A	GBF4	nd[b]	AtbZIP68	At1g32150	G	.	YES
AtbZIP35	At1g49720	A	ABF1	YES	AtbZIP55	At2g46270	G	GBF3	YES
AtbZIP39	At2g36270	A	ABI5	nd	AtbZIP54	At4g01120	G	GBF2	YES
AtbZIP12	At2g41070	A	DPBF4	YES	AtbZIP41	At4g36730	G	GBF1	YES
AtbZIP67	At3g44460	A	DPBF2	YES	AtbZIP56	At5g11260	H	HY5	YES
AtbZIP66	At3g56850	A	AREB3	YES	AtbZIP69	At1g06070	I	.	nd
AtbZIP37	At4g34000	A	ABF3	YES	AtbZIP52	At1g06850	I	.	nd
AtbZIP13	At5g44080	A	.	nd	AtbZIP51	At1g43700	I	VIP1	nd
AtbZIP17	At2g40950	B	.	nd	AtbZIP59	At2g31370	I	PosF21	nd
AtbZIP28	At3g10800	B	.	nd	AtbZIP18	At2g40620	I	.	nd
AtbZIP25	At3g54620	C	.	nd	AtbZIP29	At4g38900	I	.	nd
AtbZIP9	At5g24800	C	BZO2H2	nd	AtbZIP44	At1g75390	S	.	YES
AtbZIP63	At5g28770	C	.	nd	AtbZIP2	At2g18160	S	GBF5	YES
AtbZIP22	At1g22070	D	TGA3	nd	AtbZIP6	At2g22850	S	.	nd
AtbZIP46	At1g68640	D	Perianthia	nd	AtbZIP53	At3g62420	S	.	YES
AtbZIP50	At1g77920	D	.	YES	AtbZIP11	At4g34590	S	GBF6	YES
AtbZIP20	At5g06950	D	TGA2	YES	AtbZIP3	At5g15830	S	.	YES
AtbZIP26	At5g06960	D	TGA5	YES	AtbZIP1	At5g49450	S	.	nd
AtbZIP57	At5g10030	D	TGA4	YES	AtbZIP62	At1g19490	—	.	nd
AtbZIP47	At5g65210	D	TGA1	YES	AtbZIP60	At1g42990	—	.	nd
AtbZIP34	At2g42380	E	.	nd					
AtbZIP61	At3g58120	E	.	nd					
AtbZIP23	At2g16770	F	.	nd					
AtbZIP24	At3g51960	F	.	nd					
AtbZIP19	At4g35040	F	.	nd					

[a]group
[b]not detected

D, G, H, and S in the bZIP family with DNA sequences containing the ACGT core was confirmed (Table 1). On the other hand, no binding of group C proteins was observed. It has been reported that group C proteins in the bZIP family have conserved phosphorylation sites,[8] and that a maize group C bZIP protein, Opaque2, is modified by phosphorylation.[15] Hence group C proteins may need some modification such as phosphorylation for binding.

Transcription is controlled by binding of TFs to the transcription regulatory region (TRR) in the 5′-upstream region of a gene. Thus, for better understanding of the gene expression network, it is important to analyze the binding of a TF to the TRR of a gene. Initiation of flowering is regulated by many genes. Among these, the *FLC* and *LFY* genes are known to be important negative and positive regulators respectively.[16,17] Next we used the upstream regions of the *FLC* (At5g10140) and *LFY* (At5g61850) genes as the target TRR sequences and searched for the TFs binding to these TRRs. For this purpose, biotinylated target TRR fragments containing the respective 5′-regulatory regions (300 bp, encompassing the −450 to −150 bp upstream region from the start codon of each gene) were generated by PCR using 5′-biotin-labeled primers, and randomly selected 192 TFs were synthesized by a cell-free protein synthesis system using [^{14}C]leucine. We divided the ^{14}C-labeled TFs into eight groups, each of which contained 24 different TFs. Each group of TFs was then mixed and incubated with one of the biotin-labeled target TRR fragments. After incubation, the target TRR fragments were pulled down using streptavidin-conjugated magnetic beads. The beads were washed 3 times and then subjected to SDS–PAGE analysis. In our search for the TFs binding to the *FLC* TRR fragment, specific binding of a 44 kDa protein to the fragment was observed in a TF group (data not shown). Among the 24 TFs that were mixed and used in the binding assay in the group, three TFs had predicted molecular masses of about 44 kDa. The binding activities of these three candidates to the *FLC* fragment were individually examined by competition assay. The candidate proteins were incubated with a biotinylated *FLC* fragment in the presence and the absence of a non-labeled competitor DNA fragment, and finally the At3g12720 product (MYB67) was found bind specifically to the TRR region of the *FLC* gene (Fig. 1C). Following the same assay protocol, a protein synthesized from clone At4g36730 (G-box binding factor 1, GBF1) was found to be a specific binding protein for the *LFY* TRR fragment (Fig. 1C). MYB67 and GBF1 belong to the MYB and bZIP families respectively. Typical binding sequences for MYB ((C/T)AAC(T/G)G) and bZIP (G-box: CACGTG) TFs do not exist in TRR fragments used in these experiments, but similar sequences, TAAATG (−314 to −319) and CACATT (−201 to −206), were found in the *FLC* and *LFY* TRR fragments respectively. Binding of GBF1 to CACATT in the *LFY* TRR fragment was confirmed by DNA foot-printing analysis (data not shown). Although further experiments are required to determine whether MYB67 and GBF1 do in fact bind to those sequences in *FLC* and *LFY* TRR respectively *in vivo*, these results suggest that our TF protein library may help in large-scale screening for isolation of TFs that bind to the TRR of target genes. Furthermore, the result that a bZIP TF, GBF1, binds to a sequence not identical to the A-, C-, or G-boxes suggests that the bZIP TFs for which we did not detect binding activity with the A-, C-, or G-boxes in this study might also recognize similar sequences to those elements.

For genome-wide biochemical analysis, large-scale synthesis of proteins has so far been a technological bottleneck. Methodologically, it is impossible to achieve genome-scale synthesis of proteins by conventional methods using living cells. In contrast, our cell-free protein synthesis system from wheat embryo is very suitable for the large-scale production of proteins. We created a protein library consisting of 647 Arabidopsis TFs using the cell-free system in this study. Using the TF library, we demonstrated DNA-binding assay of bZIP TFs and screening of TF binding to the TRR of *FLC* and *LFY*. These results indicate that the quality of the protein library is sufficient for large-scale biochemical characterization. The cell-free based protein library might become a promising tool in genome-wide biochemical analysis. Recently, we also succeeded in establishing a protein microarray system based on this cell-free protein synthesis system.[18] We hope that appropriate use of these methods will accelerate the progress of the genome-wide biochemical analysis of proteins.

Acknowledgments

This work was partially supported by the program of Special Coordination Funds for Promoting Science and Technology of the Ministry of Education, Culture, Sports, Science, and Technology of Japan (financial support to T.S. and Y.E.).

References

1) International Human Genome Sequencing Consortium, *Nature*, **409**, 860–921 (2001).
2) Riechmann JL, Heard J, Martin G, Reuber L, Jiang CZ, Keddie J, Adam L, Pineda O, Ratcliffe OJ, Samaha RR, Creelman R, Pilgrim M, Broun P, Zhang JZ, Ghandehari D, Sherman BK, and Yu GL, *Science*, **290**, 2105–2110 (2000).
3) Madin K, Sawasaki T, Ogasawara T, and Endo Y, *Proc. Natl. Acad. Sci. USA*, **97**, 559–564 (2000).
4) Sawasaki T, Ogasawara T, Morishita R, and Endo Y, *Proc. Natl. Acad. Sci. USA*, **99**, 14652–14657 (2002).
5) Seki M, Narusaka M, Kamiya A, Ishida J, Satou M, Sakurai T, Nakajima M, Enju A, Akiyama K, Oono Y, Muramatsu M, Hayashizaki Y, Kawai J, Carninci P, Itoh M, Ishii Y, Akazawa T, Shibata K, Shinagawa A, and Shinozaki K, *Science*, **296**, 141–145 (2002).
6) Sawasaki T, Morishita R, Gouda MD, and Endo Y, *Methods Mol. Biol.*, **375**, 95–106 (2007).
7) Sawasaki T, Hasegawa Y, Tsuchimochi M, Kamura N, Ogasawara T, Kuroita T, and Endo Y, *FEBS Lett.*, **514**, 102–105 (2002).
8) Jakoby M, Weisshaar B, Droge-Laser W, Vicente-Carbajosa J, Tiedemann J, Kroj T, and Parcy F, *Trends Plant Sci.*, **7**, 106–111 (2002).
9) Izawa T, Foster R, Nakajima M, Shimamoto K, and Chua NH, *Plant Cell*, **6**, 1277–1287 (1994).
10) Kobayashi T, Kodani Y, Nozawa A, Endo Y, and Sawasaki T, *FEBS Lett.*, **582**, 2737–2744 (2008).
11) Lara P, Oñate-Sánchez L, Abraham Z, Ferrándiz C, Díaz I, Carbonero P, and Vicente-Carbajosa J, *J. Biol. Chem.*, **278**, 21003–21011 (2003).
12) Satoh R, Fujita Y, Nakashima K, Shinozaki K, and Yamaguchi-Shinozaki K, *Plant Cell Physiol.*, **45**, 309–317 (2004).
13) Lee SS, Yang SH, Berberich T, Miyazaki A, and Kusano T, *Plant Biotechnol.*, **23**, 249–258 (2006).
14) Kaminaka H, Näke C, Epple P, Dittgen J, Schütze K, Chaban C, Holt III BF, Merkle T, Schäfer E, Harter K, and Dangl JL, *EMBO J.*, **25**, 4400–4411 (2006).
15) Ciceri P, Gianazza E, Lazzari B, Lippoli G, Genga A, Hoschek G, Schmidt RJ, and Viotti A, *Plant Cell*, **9**, 97–108 (1997).
16) Alexandre CA and Hennig L, *J. Exp. Bot.*, **59**, 1127–1135 (2008).
17) Sablowski R, *J. Exp. Bot.*, **58**, 899–907 (2007).
18) Sawasaki T, Kamura N, Matsunaga S, Saeki M, Tsuchimochi M, Morishita R, and Endo Y, *FEBS Lett.*, **582**, 221–228 (2008).

Journal of Experimental Botany, Vol. 60, No. 11, pp. 3067–3073, 2009
doi:10.1093/jxb/erp134 Advance Access publication 8 May, 2009
This paper is available online free of all access charges (see http://jxb.oxfordjournals.org/open_access.html for further details)

Journal of Experimental Botany
www.jxb.oxfordjournals.org

RESEARCH PAPER

Isolation and identification of ubiquitin-related proteins from *Arabidopsis* seedlings

Tomoko Igawa[1,*], Masayuki Fujiwara[1], Hirotaka Takahashi[2], Tatsuya Sawasaki[2], Yaeta Endo[2], Motoaki Seki[3], Kazuo Shinozaki[3], Yoichiro Fukao[1] and Yuki Yanagawa[1,*,†]

[1] The Plant Science Education Unit, The Graduate School of Biological Sciences, Nara Institute of Science and Technology, 8916-5 Takayama-cho, Ikoma, Nara 630-0101, Japan
[2] Cell-Free Science and Technology Research Center, Ehime University, 3 Bunkyo-cho, Matsuyama, Ehime 790-8577, Japan
[3] RIKEN Bioresource Center, 3-1-1 Takayama-cho, Tsukuba, Ibaraki 305-0074, Japan

Received 15 December 2008; Revised 9 March 2009; Accepted 6 April 2009

Abstract

The majority of proteins in eukaryotic cells are modified according to highly regulated mechanisms to fulfill specific functions and to achieve localization, stability, and transport. Protein ubiquitination is one of the major post-translational modifications occurring in eukaryotic cells. To obtain the proteomic dataset related to the ubiquitin (Ub)-dependent regulatory system in *Arabidopsis*, affinity purification with an anti-Ub antibody under native condition was performed. Using MS/MS analysis, 196 distinct proteins represented by 251 distinct genes were identified. The identified proteins were involved in metabolism (23.0%), stress response (21.4%), translation (16.8%), transport (6.7%), cell morphology (3.6%), and signal transduction (1.5%), in addition to proteolysis (16.8%) to which proteasome subunits (14.3%) is included. On the basis of potential ubiquitination-targeting signal motifs, in-gel mobilities, and previous reports, 78 of the identified proteins were classified as ubiquitinated proteins and the rest were speculated to be associated proteins of ubiquitinated proteins. The degradation of three proteins predicted to be ubiquitinated proteins was inhibited by a proteasome inhibitor, suggesting that the proteins were regulated by Ub/proteasome-dependent proteolysis.

Key words: *Arabidopsis* seedling, MS, ubiquitin-related protein.

Introduction

Ubiquitin (Ub)-mediated protein modification is a critical post-translational regulatory mechanism that occurs in all eukaryotic cells. The conserved 76 amino acid polypeptide, Ub, is covalently attached to a substrate protein as a signal molecule, and this attachment leads to various outcomes. The widely known fate of ubiquitinated proteins is degradation by 26S proteasome, one specific case being that more than four Ubs comprise a multi-Ub chain via lysine (K) 48 residues (Thrower *et al.*, 2000). Other types of ubiquitination, such as mono-ubiquitination and non-canonical ubiquitination, are implicated in various cellular functions, including endocytosis, endosomal sorting, signal transduction, and DNA damage repair (reviewed by Haglund and Dikic, 2005). Ubiquitination of target proteins requires the sequential action of three enzymes: Ub-activating enzyme (E1), Ub-conjugating enzyme (E2 or UBC), and Ub ligase (E3) (Hershko and Ciechanover, 1998; Pickart, 2001). The completely sequenced *Arabidopsis* genome has enabled the prediction of plant ubiquitination enzymes. To date, the activities of two E1s (Hatfield *et al.*, 1997) and 25 E2s (Kraft *et al.*, 2005) have been experimentally proven, and 12 genes encoding UBC domains are predicted to be E2s on the basis of their sequences (Bachmair *et al.*, 2001). Similar to other organisms, *Arabidopsis* E3s are predicted to form the largest

* These authors contributed equally to this work.
† To whom correspondence should be addressed: E-mail: yyana@bs.naist.jp
Abbreviations: DET3, de-etiolated 3; FBA, fructose biphosphate aldolase-like; GAPC, glyceraldehyde-3-phosphate dehydrogenase C subunit; ORF, open reading frame; Ub, ubiquitin; V-ATPase, vacuolar H^+-ATPase.

family comprising more than 1400 genes (Mazzucotelli *et al.*, 2006). Furthermore, the presence of additional proteins, such as an enhancer of E2, has been reported (Yanagawa *et al.*, 2004). Clearly, numerous proteins are involved in Ub-mediated protein regulation.

To identify ubiquitinated proteins in yeasts and mammals, several proteomic approaches that utilize various purification methods and MS/MS analyses have been reported (Peng *et al.*, 2003; Hatakeyama *et al.*, 2005; Jeon *et al.*, 2007). In plants, two groups recently reported the proteomics of ubiquitinated proteins from *Arabidopsis* cell cultures and seedlings, respectively (Maor *et al.*, 2007; Manzano *et al.*, 2008). Meanwhile, a Ub-related proteome that includes both ubiquitinated proteins and their associated proteins has been reported only in human cells (Matsumoto *et al.*, 2005).

As many proteins show spatiotemporal expression during development/life cycle, it is speculated that Ub-related proteins also vary among distinct tissues at various developmental stages. Therefore, the accumulation of information of Ub-related proteins from differentiated tissues at various stages would facilitate an understanding of Ub-mediated protein regulation throughout the life cycle. In addition, to make a comparison with the reports of Maor *et al.* (2007) and Manzano *et al.* (2008) that provided useful information of ubiquitinated proteomes from non-differentiated cell cultures and *Arabidopsis* seedlings, respectively, the proteomic analysis of Ub-related proteins expressed in *Arabidopsis* seedlings was performed in this study. For the large-scale isolation of Ub-related proteins, the purification was performed under native conditions. Previous studies of *Arabidopsis* ubiquitinated proteomes utilized different Ub-binding domains (UBAs) and showed that each UBA has distinct specificity for ubiquitinated proteins (Maor *et al.*, 2007; Manzano *et al.*, 2008). In order to overcome the limited specificity for target recognition, an anti-Ub antibody was applied to isolate Ub-related proteins. This study could provide helpful information for future work related to Ub-mediated protein regulation in plants.

Materials and methods

Plant materials

Arabidopsis (ecotype Columbia) seeds were germinated and cultured with shaking in liquid Murashige and Skoog medium containing 1% sucrose and 0.5 g l^{-1} MES, under a 16/8 h light/dark cycle at 22 °C. MG132 (Peptide Institute, Inc., Osaka, Japan) was added to 10-d-old cultured seedlings at a final concentration of 10 μM. After 24 h treatment, the seedlings were harvested. *Nicotiana benthamiana* was grown in a temperature-controlled growth room maintained at 25 °C under a 16/8 h light/dark cycle. Four- to five-week-old plants were used for experiments.

Large-scale purification of Ub-related proteins

To prepare an immunoaffinity column, HiTrap NHS-activated HP (1 ml, GE Healthcare Amersham Biosciences KK, Tokyo, Japan) was coupled with 1 mg of anti-Ub antibody FK2 (Nippon Bio-Test Laboratories, Tokyo, Japan) or mouse serum (Chemicon International, Inc., California, USA) as a negative control according to the manufacturer's instructions.

To purify Ub-related proteins under native condition, *Arabidopsis* seedlings were ground in liquid N_2 with a mortar and pestle, and the powder was further ground in buffer A [50 mM TRIS-HCl (pH 7.5), 150 mM NaCl] containing the Complete Protease Inhibitor cocktail (Roche Applied Science, GmbH, Mannheim, Germany), 5 mM 2-mercaptoethanol, and 10 μM MG132. The homogenate was centrifuged at 32 300 *g* for 15 min and the supernatant was centrifuged again for 5 min. The supernatant was filtered through a 0.8 μm syringe filter. The total protein extract (200–250 mg) was applied to an immunoaffinity column equilibrated with buffer A. After washing the column with 5 vols of buffer A, bound proteins were eluted with buffer B [0.1 M glycine-HCl (pH 3.0), 150 mM NaCl]. Purification of the Ub-related proteins was performed three times.

In-gel digestion of purified proteins, MS/MS analysis, and data reduction

The eluted proteins from three independent purifications were mixed and fractionated by SDS-PAGE. Protein bands were detected with Flamingo™ Fluorescent Gel Stain (Bio-Rad Laboratories, CA, USA). The protein bands were excised and other smearing regions were cut into 2-mm-long gel pieces for in-gel trypsin digestion. In-gel digestion and MS/MS analysis were performed according to the methods described by Fujiwara *et al.* (2006) and Nakashima *et al.* (2008). The gel pieces were dehydrated by washing twice with 100% acetonitrile, and dried with a vacuum concentrator. The proteins were reduced with 10 mM DTT at 56 °C for 45 min and then alkylated with 55 mM iodoacetamide at room temperature in the dark for 30 min. After washing twice with 25 mM ammonium bicarbonate, the samples were dehydrated again with 50% acetonitrile and dried. The protein samples were digested with 10 μg ml^{-1} proteomics-grade trypsin (Promega, Madison, WI, USA) for 12 h at 37 °C.

The digested peptides were subjected to column chromatography (PEPMAPC18, 5 μm, 75 μm internal diameter, 15 cm; Dionex, Sunnyvale, CA) using the CapLC system (Waters, Milford, MA, USA). Buffers were 0.1% formic acid in water (A) and 0.1% formic acid in acetonitrile (B). A linear gradient from 5% to 45% B for 25 min was applied, and peptides eluted from the column were introduced directly into a Q-TOF Ultima mass spectrometer (Waters) at a flow rate of 100 nl min^{-1}. In the ESI-positive ion mode, ionization was performed at a capillary voltage of 2.2 kV with the PicoTip nanospray source (New Objective, Cambridge, MA). For survey scan, mass spectra were acquired for the two most intense ions from the precursor ion scan between m/z 400 and 1500. For collision-induced dissociation (CID), the collision energy was set automatically according to the mass and charge state of the precursor peptide. MS/MS spectra were analysed with the MASCOT server against a protein database from the